UNIVERSITY OF PARDUBICE

FACULTY OF CHEMICAL TECHNOLOGY

Department of Physical Chemistry

Daniela Brandová

Crystallization Behavior of Far-Infrared Chalcogenide Glasses

Theses of the Doctoral Dissertation

Pardubice 2019

Study program: **Physical Chemistry**

Study field: **Physical Chemistry**

Author: **Daniela Brandová**

Supervisor: **prof. Ing. Jiří Málek, DrSc.**

Year of the defense: 2019

References

BRANDOVÁ, Daniela. *Crystallization Behavior of Far-Infrared Chalcogenide Glasses*. Pardubice, 2019. 303 pages. Dissertation thesis (PhD.). University of Pardubice, Faculty of Chemical Technology, Department of Physical Chemistry. Supervisor prof. Ing. Jiří Málek, DrSc.

Abstract

The doctoral thesis presents a detailed characterization of thermal and structural properties of the selected tellurium-based chalcogenide glasses. The thermal behavior of investigated glassy systems is characterized by means of differential scanning calorimetry (DSC) and thermomechanical analysis (TMA; selected systems). In the presented doctoral thesis a systematic approach to the description of complex crystallization (and relaxation) kinetics by means of the commonly used and state-of-art methodologies and models is adopted in order to achieve full description of the observed phenomena and provide the possibility of accurate kinetic predictions. The observed complexity of crystallization processes of all investigated systems is solved by means of two approaches, i.e. the mathematic deconvolution and kinetic deconvolution of the crystallization DSC data. The advantages and disadvantages of both tested methods are discussed. In addition, the observed thermal behavior of studied systems is correlated with the structural information provided by XRD analysis, Raman spectroscopy and infrared (IR) microscopy. Thermal stability of the prepared glasses is thoroughly analyzed. Combination of the calorimetric and thermo-mechanical data allows precise and reliable determination of the true glass temperature workability window.

Abstrakt

Předkládaná dizertační práce představuje detailní studii termických a strukturních vlastností vybraných teluridových chalkogenidových skel. Tyto skelné materiály patří mezi slibné ale pouze výjimečně zkoumané materiály, jež mohou potenciálně představovat materiály vhodné pro optické aplikace operující ve vzdálené oblasti infračerveného spektra a sklokeramiku. Termické chování studovaných systémů je charakterizováno pomocí diferenční skenovací kalorimetrie (DSC) a termomechanické analýzy (TMA; vybrané systémy). V předložené dizertační práci je osvojen systematický přístup k popisu komplexní krystalizační (a relaxační) kinetiky prostřednictvím běžně užívaných i nejmodernějších metodologií a modelů za účelem dosažení úplného popisu pozorovaných jevů a poskytnutí možnosti přesných kinetických predikcí. Pozorovaná komplexita krystalizačního procesu všech zkoumaných systémů je řešena s využitím dvou přístupů, a to matematické a kinetické dekonvoluce krystalizačních DSC dat. Výhody a nevýhody obou metod jsou diskutovány. Kromě toho je termické chování studovaných systémů korelováno se strukturní informací získané z rentgenové difrakční analýzy, Ramanovy spektroskopie a infračervené mikroskopie. Tepelná stabilita připravených skel je důkladně analyzována. Kombinace kalorimetrických a termomechanických dat umožňuje přesné a spolehlivé určení skutečného teplotního okna pro zpracování skla.

Keywords
crystallization kinetics; chalcogenide glass; glass stability; DSC; TMA; XRD; Raman spectroscopy; infrared microscopy

Klíčová slova
kinetika krystalizace; chalkogenidové sklo; skelná stabilita; DSC; TMA; XRD; Ramanova spektroskopie; infračervená mikroskopie

Table of Contents

Introduction

Chalcogenide glasses belong to the technologically important and interesting materials due to their unique properties (e.g. high transmittance in the infrared region of the electromagnetic spectrum, semiconducting properties, high refractive index – higher than SiO_2-based glass, etc.), thus these materials are widely used as large capacity data-storage media (CDs, DVDs, BlueRay Discs or non-volatile PCRAMs), elements for infrared optics (fibers, lenses, etc.), optoelectronics, memory switches or various electronic thresholds. [1,2]

One of the promising chalcogenide materials is tellurium-based glass. These systems are well-known for their excellent transmittance in the infrared (IR) region. The transmittance window can range from 2 up to 28 μm; it depends on the exact composition. This feature can be successfully utilized in various hi-tech IR applications including biosensors with usage in medicine or environmental sphere [3], CO_2 detectors fighting the global warming [4], space optics detecting the biological life markers (such as absorption bands of CO_2, O_3, H_2O) on exoplanets [5-7]. The great disadvantage of telluride glasses is their high tendency towards crystallization, which results in complications in the further processing of the glassy material. Each of all processing steps must then be strictly controlled to prevent the possible crystallization. Nowadays, the great emphasis is placed to the search of the material with appropriate thermal, optical and compositional properties. The main goal is then to achieve the highest thermal stability of telluride glasses while the best optical properties will be kept. The resulting knowledge of ongoing kinetic processes, thermal properties and structural arrangement may serve to predict the behavior of the material for arbitrary conditions that can be used in finding the new hi-tech materials, technology for the glass-preparation or usage of these glasses in commercial applications. [3-14]

1 Theory

1.1 Glass formation

The reversible transition, when the undercooled liquid (during further cooling) has been getting into a thermodynamically non-equilibrium glassy state, is called the glass transition. A liquid above its melting point represents the initial state; when the cooling begins, most materials start to solidify, crystallization occurs and these processes are connected with discontinuous change of volume, enthalpy, Gibbs energy, etc. This can be avoided by a sufficiently rapid cooling of the melt/liquid, the material does not have enough time for the nucleation and subsequent crystal growth, leaves the liquid state and changes to a mechanically rigid system – the glass. The viscosity of the system within the cooling process gradually increases until the value equals approx. 10^{12} Pa.s – at this moment the glass is formed. Nonetheless, the glassy structure has still remained disordered and has kept the liquid-like structure. This process is characterized by continuous change of the volume, enthalpy, Gibbs energy, while the discontinuity in the second derivative of Gibbs energy occurs, i.e. in the temperature dependence of heat capacity c_p, coefficient of thermal expansion α_{exp},

compressibility β_c. The Gibbs energy values representing the system in glassy state are higher than values corresponding to the crystalline state.

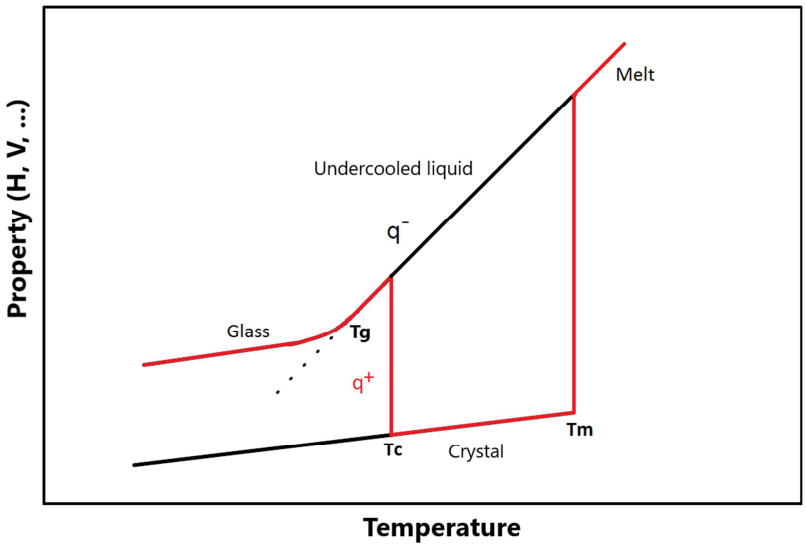

Figure 1: The temperature dependence of given property (H, V, …) in the glass transition area; corresponding temperatures are displayed; q^- represents the cooling rate, q^+ represents the heating rate.

The glass formation is demonstrated as a departure from the equilibrium with the decrease of property-temperature dependence slope on temperature dependence of given property. The temperature corresponding to this departure is referred as a glass transition temperature T_g. The glass transition temperature is a very important parameter determining the properties and behavior of the resulting glass. Above this temperature, the system behaves like a melt, becomes more formable; under this temperature the system behaves like a solid with a rigid structure. The glass transition temperature is not a thermodynamic quantity. This means that its value is influenced, for example, by the method of glass preparation (cooling rate q^-). At higher cooling rate, the curve corresponding to the glassy state on the temperature dependence of the given property deviates earlier, i.e. at a higher temperature, compared to a slower cooling rate. The red-labeled curve in Fig. 1 corresponds to the so-called cold crystallization process, when the glass is heated by applied heating rate (q^+), above the T_g, the structure of glass is more loosened and at the crystallization temperature T_c, the crystallization occurs, the crystalline network is formed. With the increasing temperature, the melting of crystalline structure realizes, which is characterized by a melting temperature T_m. [2,15-17]

1.1.1 Structural relaxation in glasses

The glass transition is not a thermodynamically controlled process due to its dependence on actual experimental conditions. Therefore it means that the glass transition process is kinetically controlled. If the undercooled liquid is sufficiently cooled and the glass is formed, the non-equilibrium glassy state endeavors to reach the equilibrium. This process is known as a structural relaxation and is associated with slow molecular rearrangement. In a consequence of the structural relaxation processes,

the glassy structure becomes more and more compact. The state to which the glassy structure relaxes is the state of the undercooled liquid (extrapolated to a given temperature range), which represents the “equilibrium state” when the glasses and glass-forming processes are under consideration. Here, the system is in the so-called kinetic equilibrium, i.e. the high energy/kinetic barriers hinder the further decrease and transformation to the crystalline state. Certainly, these structural changes lead to several changes in physical properties, for example optical transmittance or density. The capability of prediction or monitoring these changes plays an important role for the potential glass technology. The classification of relaxation process is based on the property, which is monitored. The two most common properties are the volume and enthalpy. [15-19]

1.2 Crystallization

The crystallization process belongs among the first-order phase transitions (according to Ehrenfest), and is characterized by a discontinuous change in temperature dependence of volume, enthalpy, entropy, etc. The atomic reorganization into a periodical crystal structure goes on, the Gibbs energy value decreases to an absolute minimum and the crystalline system reaches the thermodynamically equilibrium state. The crystalline system may be obtained by a slow cooling of a melt, when the melt material has enough time (within the cooling) to create a periodically organized system – a crystal; or the another way to acquire the crystalline products is the so-called cold crystallization including a heating of the amorphous/glassy material to its crystallization temperature. [2,16]

The crystallization could be described by two subsequent processes – the nucleation and the crystal growth. Firstly, the new-phase nuclei are created, the amount and size of nuclei steadily increases simultaneously. This process is called nucleation and may proceed with two different mechanisms – homogeneous or heterogeneous nucleation. In the first case, the nuclei emerge randomly throughout the volume of melt, solid or crystal; in the second case, the nuclei originate at energy-efficient/preferred locations (such as defects, inclusions, dislocations, additive atoms), which function as crystallization centers; the magnitude of the energy barrier is in most cases several orders less than in case of homogenous nucleation. [2,16,18,19,21] Subsequently, the crystal growth follows and includes two important processes – the mass transport to and via the newly-emerged phase interface. The studies focused on a description of crystal growth may be performed with utilization of two approaches – the direct microscopic observation with using the microscopic methods (optical, electron microscopy) and three basic phenomenological models (normal growth, screw dislocation growth, two-dimensional surface nucleated growth models [22,23]); or the usage of indirect macroscopic observation of crystallization. This method is based on thermal analysis, which can be realized by means of differential thermal analysis (DTA), differential scanning calorimetry (DSC) and also by means of thermomechanical analysis (TMA). [2,15-19,21,24,25]

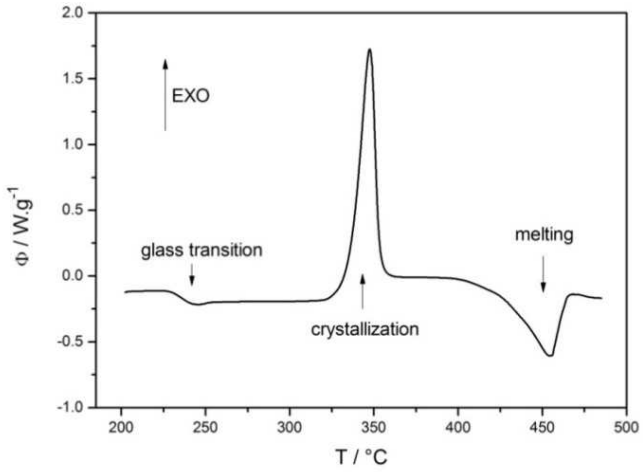

Figure 2: The example of DSC curve observed for non-isothermal measurement; the corresponding thermal effects are denoted.

1.3 The prediction of glass stability (the glass-stability criteria)

The glass-stability (GS) criteria are widely used parameters in scientific practice to characterize and predict the behavior of amorphous/glassy materials. Further, with their knowledge, it can be estimated whether the required substance is capable to form a stable glass or not. The noticeable effort has been dedicated to the search of the most suitable GS criteria in regard to the potential real-life applications of the given glassy material.

The glass-forming criterion introduced by Zachariansen [26] represents the oldest way to assess the ability to form a glass. This criterion works on the assumption of the structural preconditions of studied systems. However, there is a certain limitation. It is necessary to know the structure of the emerging glass, which is not always possible, primarily in case of the newly studied systems.

The thermodynamic approach of glass-stability evaluations is based on e.g. the bond energy determinations, the differences in the electronegativity of constituent elements, the relations between the characteristic temperatures - glass transition temperature T_g, crystallization temperature T_c (onset vs. maximum of the signal) and melting temperature T_m and their ratios. [2,27] The last mentioned GS criteria based on relations between the characteristic temperatures have an advantage in their relative simplicity (due to their evaluation) and good functionality in series of chemically resembling glasses. The most common used GS criteria include the criteria defined by Hruby K_H [28], Saad and Poulain K_{SP} [29], Weinberg K_W [30], Lu and Liu K_{LL} [31], Long K_{LX} [32], and Zhang K_{ZW} [33]. As the most suitable criterion (for chalcogenide materials) was found the Hruby criterion (see Ref. [34]) that manifested the lowest normalized variability with the experimental conditions in contrary to K_W, K_{LL}, K_{LX} and K_{ZW}. The large influence of experimental conditions (such as a sample form, heating rate, the way of determination of each characteristic temperature, i.e. onset vs. signal maximum) on these criteria is obvious. Nonetheless, the difference between the glass transition temperature T_g and the crystallization

temperature T_c has still remained crucial. The wider the difference T_g - T_c, the more stable the glass is. In scientific practice the so-called ΔT criterion ($\Delta T = T_c - T_g$) [8-10] is used to consider the thermal stability of the given glassy system.

The last (but not least) way to characterize the glass stability represents the kinetic models. This alternative approach (with regard to thermodynamic approach) takes into account the fact, that each material is able to form a glass, if the adequate cooling rate is applied. The initial point of considering the glass ability or stability represents the construction of T-T-T (Temperature-Time-Transformation) curves. Unfortunately, a huge amount of information is required and not all of the needed parameters are often available. That is a great limitation of applicability the kinetic models. [2,27]

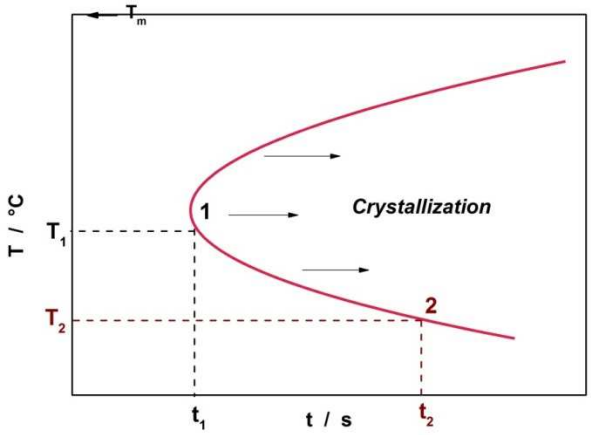

Figure 3: The illustration of T-T-T curve; the temperature and the corresponding time needed to the crystallization of given portion of glass are depicted.

1.4 Theory of kinetic analysis

The scientific research attaches importance to the study of crystallization processes occurring in glassy materials as a consequence of wide-ranging usage of these materials. If the crystallization kinetics is well-known, the predictions of the preparation conditions, potential real-life applicability and so on can be done, which enable a better control of the experimental conditions and properties of resulting glassy material. The crystallization processes in various materials may be monitored by two basic methods, namely by the direct (microscopic) and indirect (thermal analysis) observations. The usage of indirect macroscopic procedures includes the methods of thermal analysis (e. g. DTA, DSC, TMA) and is a favorite and widespread way how to obtain the valuable data about crystallization process, which are further used for e.g. an evaluation of crystallization kinetics.

The doctoral thesis is primarily focused on the study of crystallization kinetics of tellurium-based chalcogenide glasses with following appraising of the processability of investigated glassy materials. The knowledge of crystallization process kinetics is important for the preparation and further processing of glassy materials due to possibility of monitoring the individual steps, experimental conditions of glass processing and the opportunity to predict the glassy material's behavior under various optional experimental conditions. In the doctoral thesis, also the structural relaxation kinetics will be described (rather as a side-note) with respect to

the completion of predictions of the glass stability, crystallization and structural processes occurring in the studied chalcogenide systems.

1.4.1 The procedures of crystallization kinetics assessments

In glassy materials, the so-called cold crystallization including, a heating of the amorphous/glassy material to its crystallization temperature occurred. The crystallization kinetics is commonly studied by means of DSC. In the case of the heat flux DSC instrument, the temperature difference between the sample and the reference ΔT_{DSC} is measured in dependence of the sample temperature. This signal is then converted and registered as a heat flow (Φ):

$$\Phi = \frac{dH}{dT} \tag{1}$$

where H is an enthalpy, T is a temperature. The actual process rate is directly proportional to the measured heat flow. The constant of proportionality is then the overall enthalpy change ΔH (for the calibrated devices). The kinetic equation is then determined as:

$$\Phi = \Delta H \cdot \left(\frac{d\alpha}{dt}\right) \tag{2}$$

where α stands for a degree of conversion and t is a time. In the case of non-isothermal DSC measurements, the Equation (2) changes its form to the Equation (3):

$$\Phi = \Delta H \cdot \left(\frac{d\alpha}{dT}\right) \cdot \left(\frac{dT}{dt}\right) \tag{3}$$

If the kinetic analysis is required, a kinetic dataset needs to be prepared. The kinetic dataset contains points and each of these points is characterized by the values of temperature (T), heat flow related to the sample weight (Φ, $W.g^{-1}$) and degree of conversion (α) (see the Equation (4)). [35-38]

$$\alpha_j = \frac{1}{\Delta H} \cdot \int_{T_0}^{T_j} \Phi \cdot dT \tag{4}$$

The kinetic analysis of DSC data is based on the search of the most suitable kinetic model that facilitates an appropriate description of a given kinetic process. If the separation of thermal and rate component of the kinetic equation is possible, the relation characterizing the actual process rate is estimated as:

$$\frac{d\alpha}{dt} = K(T) \cdot f(\alpha) \tag{5}$$

where $\frac{d\alpha}{dt}$ stands for reaction/transformation rate, K(T) is a rate constant (depends on temperature) and f(α) denotes an expression of suitable kinetic model (α is a conversion).

The rate constant can be expressed by using the known Arrhenius equation:

$$K(T) = A \cdot e^{-\frac{E_A}{RT}} \tag{6}$$

where A is a preexponential factor, E_A is an apparent activation energy of the studied process, R is an universal gas constant, T is a temperature. The kinetic analysis of DSC data is realized by means of the DSC universal kinetic equation (see Eq. (7)), which has arisen by the conjunction of above-mentioned equations (2), (5), (6). Thus, the DSC universal kinetic equation is determined as:

$$\Phi = \Delta H \cdot A \cdot e^{-\frac{E_A}{RT}} \cdot f(\alpha) \tag{7}$$

The common kinetic models, which can serve as a description of crystallization kinetics of data provided by DSC, are for example the nucleation-growth Johnson-Mehl-Avrami (JMA(m)), autocatalytic Šesták-Berggren (AC(M,N)), reaction order (RO(n)), diffusion (D1-3), Ginstling-Brounshtein (D4), contracting area (R2) or contracting volume (R3) models. The kinetic models represent a theoretical (mathematical) characterization of studied processes, which experimentally occur in given materials. The Table 1 offers the summary of chosen kinetic models, their labeling and corresponding forms of f(α) functions. [20,26,27,39,40]

Table 1: Kinetic models

Model	Symbol	f(α)
Johnson-Mehl-Avrami	**JMA(m)**	$\boldsymbol{m(1-\alpha)[-\ln(1-\alpha)]^{1-\frac{1}{m}}}$
Autocatalytic Šesták-Berggren	**AC(M,N)**	$\boldsymbol{\alpha^M(1-\alpha)^N}$
Reaction order	**RO(n)**	$\boldsymbol{(1-\alpha)^n}$
1-D diffusion	**D1**	$\boldsymbol{\frac{1}{2\alpha}}$
2-D diffusion	**D2**	$\boldsymbol{-[1/\ln(1-\alpha)]}$
3-D diffusion (Jander)	**D3**	$\boldsymbol{\left[3(1-\alpha)^{\frac{2}{3}}\right] / \left[2(1-(1-\alpha)^{\frac{1}{3}})\right]}$
Ginstling-Brounshtein	**D4**	$\boldsymbol{3/\left[2((1-\alpha)^{-\frac{1}{3}}-1)\right]}$
Contracting area	**R2**	$\boldsymbol{2(1-\alpha)^{\frac{1}{2}}}$
Contracting volume	**R3**	$\boldsymbol{3(1-\alpha)^{\frac{2}{3}}}$

The activation energy determination

The first step of kinetic analysis of experimental DSC crystallization data represents the determination of the activation energy of crystallization. Nowadays, there are several methods developed for this purpose, firstly the Kissinger [41] method, further the Friedman [42] and Kissinger-Akahira-Sunose (KAS) [43] methods.

The Kissinger method is simple and is based on the temperature shift of the DSC signal maximum, which is associated with different applied heating rates. The usage of this method therefore consists in case of non-isothermal measurements. The Equation (8) depicts the principle of Kissinger method, where q^+ stands for heating rate and T_p is the temperature corresponding to the maximum of the crystallization peak. The value of the activation energy is derived from the slope of the linear dependence $ln\left(\frac{q^+}{T_p^2}\right)$ vs. $\frac{10^3}{T_p}$.

$$ln\left(\frac{q^+}{T_p^2}\right) = const. - \frac{E_A}{RT_p} \quad (8)$$

Some limitations of usage this method for evaluation the activation energy of crystallization exist. For example, the Kissinger method provides only the E_A single value (representing the dominant crystallization process), which can make the difficulties in an assessment of complex processes, which contain more than one crystallization process. [35,44-47]

The Friedman and KAS methods belong to a group of isoconversional methods. These procedures are based on the assumption that the reaction rate in the constant conversion range is only temperature dependent. The degree of conversion remains constant, so the reaction or phase transformations do not vary with changing heating rate. Thus, the values of E_A are estimated as an average of E_A values determined for chosen degrees of conversion. This procedure leads to the minimization of the influence of experimental conditions. These methods are usable for non-isothermal and also for isothermal measurements. [42,47-50]

The Friedman method is a differential isoconversional method of E_A evaluation and is expressed by the Equation (9):

$$\ln(\Phi_\alpha) = const. - \frac{E_A}{RT_\alpha} \quad (9)$$

where Φ_α, T_α are a heat flow and temperature corresponding to the chosen values of conversion; the interval of α values is defined as $0.3 \leq \alpha \leq 0.7$.

The integral isoconversional methods are based on the application of the isoconversional principles to the equations in the integral form. The modified KAS method is expressed by means of the Equation (10):

$$ln\left(\frac{q^+}{T_\alpha^{1.92}}\right) = const. - 1.0008\frac{E_A}{RT_\alpha} \quad (10)$$

Starink [43] has showed, that some changes in KAS equation parameters lead to a better accuracy of the E_α values. [43,44,47]

The kinetic model and kinetic parameters determination

The second step of kinetic analysis of DSC crystallization data is the search of a suitable kinetic model, which is able to describe the studied crystallization kinetics. This can be achieved by using algorithms based on the characteristic functions y(α) and z(α) [35,44,47] derived by using a simple transformation of experimental DSC data. In case of isothermal measurements, these functions can be expressed as:

$$y(\alpha) = \Phi \tag{11a}$$
$$z(\alpha) = \Phi \cdot t \tag{11b}$$

If the DSC crystallization data were obtained at non-isothermal conditions, the functions y(α) and z(α) are determined as:

$$y(\alpha) = \Phi \cdot e^{\frac{E_A}{RT}} \tag{12a}$$
$$z(\alpha) = \Phi \cdot T^2 \tag{12b}$$

The values of y(α) and z(α) functions are usually subjected to normalization procedure in the interval <0,1>. It helps to an easier data interpretation and the influence of different experimental conditions can be eliminated. In general practice, the most common kinetic models using to the description of crystallization kinetics are the nucleation-growth JMA (m) [48-50] and autocatalytic AC(M,N) [51] models.

If the value of the degree of conversion corresponds to the maxima of the z(α) function and ranges from 0.62 to 0.64 (the preferable value of $\alpha_{max,\,z}$ equals to 0.632) the crystallization kinetics can be described by the JMA (m) model. Mathematically, the JMA (m) model can be expressed using this Equation (13):

$$f(\alpha) = m(1-\alpha)[-\ln(1-\alpha)]^{1-\frac{1}{m}} \tag{13}$$

where m stands for the kinetic exponent of JMA (m) model reflecting the respective nucleation-growth mechanisms. [44,45,48-50] The JMA (m) model is a one-parameter kinetic model and the value of kinetic parameter m can be determined from the following Equation (14) [52]:

$$m = \frac{1}{1+\ln(1-\alpha_{max,y})} \tag{14}$$

The function y(α) has to provide the maximum value ranging in the interval $0 < \alpha_{max,\,y} < \alpha_{max,\,z}$ with respect to fulfil the condition of $m > 1$. Another alternative way to determine the value of the parameter m represents the determination from the linear dependence $ln[-ln(1-\alpha)]$ vs. lnt or $ln\frac{1}{T}$. [44,45,48-52]

The autocatalytic AC(M,N) model represents the alternative way for description of crystallization kinetics, if the JMA (m) model cannot be used. This semi-empirical kinetic model has two parameters and the parameters have no physical meaning, nevertheless this model is widely used not only due to its higher flexibility to experimental data.

The AC(M,N) model is mathematically expressed as:

$$f(\alpha) = \alpha^M (1-\alpha)^N \tag{15}$$

The kinetic parameters M and N can be determined by means of two consecutive evaluations; firstly the value of $\frac{M}{N}$ ratio used to be assigned (see the Equation (16)) and secondly the value of parameter N can be estimated with using the Equation (17), where the N parameter value is determined from the value of the slope of the below depicted dependence. [44,45,51,53]

$$\frac{M}{N} = \frac{\alpha_{max,y}}{1-\alpha_{max,y}} \tag{16}$$

$$ln\left[\Phi \cdot e^{\frac{E_A}{RT}}\right] = ln(\Delta H \cdot A) + N \cdot ln\left[\alpha^{\frac{M}{N}}(1-\alpha)\right] \tag{17}$$

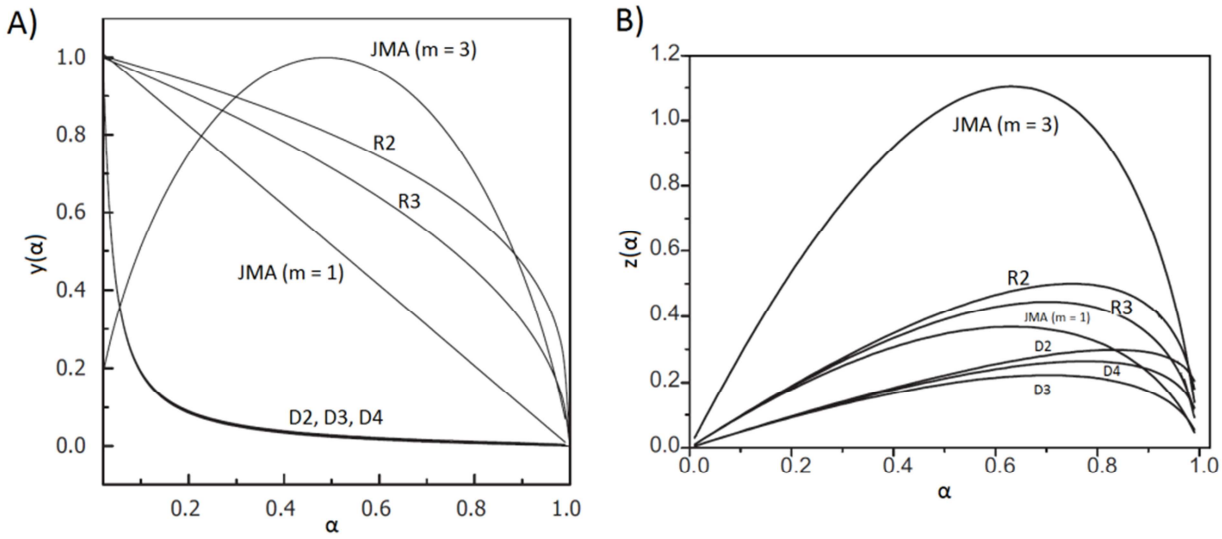

Figure 4: A), B) Schema of y(α) and z(α) plots corresponding to chosen depicted kinetic models.

The preexponential factor determination

The value of the preexponential factor A can be estimated with the knowledge of above-mentioned kinetic parameters, i.e. the activation energy value and the kinetic model and its parameters. If the crystallization kinetics is described by means of autocatalytic AC(M,N) model, the preexponential factor can be evaluated by using the above-quoted Equation (17). Another way how to obtain the A value represents the Equation (18):

$$A = -\frac{q^+ \cdot \frac{E_A}{RT}}{T \cdot f'(\alpha_{max,z})} \cdot e^{\frac{E_A}{RT}} \tag{18}$$

where $f'(\alpha_{max,z})$ stands for the differential form of kinetic model f(α). [44,45]

1.4.2 Kinetic deconvolution - Multivariate kinetic analysis (MKA)

The multivariate kinetic analysis (MKA) represents a group of model-fitting methods and many ways of model fitting exist. In general practice, the linear or non-linear regression methods can be used. These model-fitting techniques are based on the assumption of the minimization of the difference between the data, which were obtained from experimental measurements, and the calculated data. [44,54-58] The famous method of non-linear fitting techniques represents the method of least squares evaluating the data difference as the residual sum of squares (RSS) [58]:

$$RSS = \sum_{j=1}^{n} \sum_{k=First\ j}^{Last\ j} w_{j,k} \left(Y_{exp_{j,k}} - Y_{cal_{j,k}} \right)^2 \quad (19)$$

$$w_j = \frac{1}{|[d\alpha/dt]_{max}|_j + |[d\alpha/dt]_{min}|_j} \quad (20)$$

where RSS is a sum of squared residua, n is a number of measurements, j is an index of the given measurement, $First_j$ is an index of the first point of the given curve, $Last_j$ is an index of the last point of the given curve, $Y_{exp,\ j,k}$ is an experimental value of the point k of curve j, $Y_{cal\ j,k}$ is a calculated value of the point k of curve j, w_j is a weighting factor for curve j. The series of several measurements performed at different heating rates are the initial datasets, then the full-scale non-linear optimization by means of MKA proceeds and the search of the minimum of RSS by the variations of the kinetic parameters values for the individual reaction steps processes. The standard kinetic models and their mutual dependences (e.g. the parallel, consecutive, competing, reversible, independent etc. models) are usually examined and based on the best value of the correlation coefficient the suitable kinetic model can be determined. [54-58]

1.4.3 Mathematic deconvolution - Fraser-Suzuki function

Before the development of methodologies for employing the kinetic analysis equations into the complex non-linear optimization algorithms, the mathematic deconvolution was used to approximate the complex kinetics. In case of complex crystallization behavior (scenario where the crystallization peaks overlap), the beginning and the end of each single peak cannot be easily determined. The point is that the set of experimental data are separated to particular components. For this purpose, several mathematical functions exist and can be used, e.g. the Gauss [59], Lorentz [60], Weibull [61] and Fraser-Suzuki (FS) [62-65] functions. The last mentioned Fraser-Suzuki function has a great advantage consisting in it being thoroughly tested in the past – the tests confirmed that (contrary to all the other above-mentioned possibilities) the FS function can describe all kinetics readily occurring for the solid-state reactions. [62-65] The FS functions can be expressed via the Equation (21):

$$y = a_0 \cdot exp\left[-ln2 \left[\frac{\ln\left(1 + 2a_3 \cdot \frac{x - a_1}{a_2}\right)}{a_3} \right]^2 \right] \quad (21)$$

where a_0, a_1, a_2, a_3 are parameters of FS function corresponding to an amplitude, position, half-width and asymmetry of curve. The PC software PeakFit (Systat

Software Inc.) is instrumental in the processing of experimental data by means of this deconvolution procedure. [62-65]

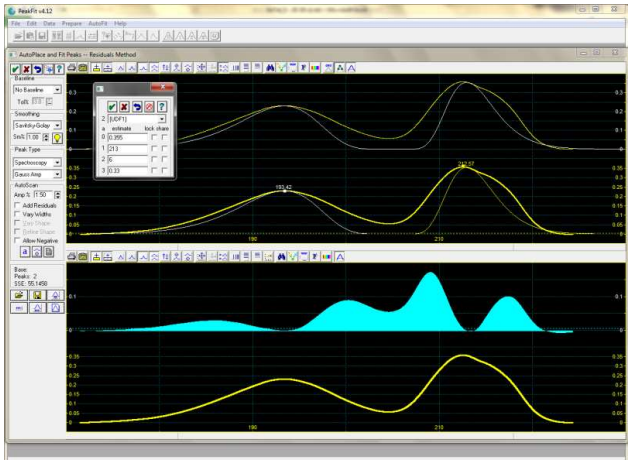

Figure 5: The illustration of deconvolution (FS) procedure with using the PC software program PeakFit 4.2 (Systat Software Inc.).

1.4.4 The structural relaxation kinetics

The glass transition is dependent on actual experimental conditions and therefore the glass transition processes are kinetically-controlled. To a description of these relaxation processes, the several kinetic models are available. Nowadays, the most common kinetic model determined for this purpose is the Tool-Narayanaswamy-Moynihan (TNM) [11,66,67] model. This phenomenological kinetic model is characterized by four parameters: the apparent activation energy Δh^* of the structural relaxation, the non-linearity parameter x, the non-exponentiality parameter β and the preexponential factor A_{TNM}, which serve to interpretation of the main relaxation features, such as hysteresis, non-linearity and non-exponentiality. The TNM model can be expressed by following Equation (22) and the next acting parameter - the fictive temperature T_f stands for the temperature of undercooled liquid with the same structure as the relaxing glass achieves and the structure of relaxing glassy material can be characterized by means of this parameter:

$$\tau = A_{TNM}\left[\frac{x\cdot\Delta h^*}{RT} + \frac{(1-x)\cdot\Delta h^*}{RT_f}\right] \tag{22}$$

The parameter x representing the non-linearity of structural relaxation determines the intensity of structure and temperature influence on relaxation process. The distribution of relaxation times is formulated by means of the Equation (23) and with using this stretched exponential function F(t) the TNM model can be implemented.

$$F(t) = exp\left[-\left(\int_0^t \frac{dt}{\tau(T,T_f)}\right)^{\beta}\right] \tag{23}$$

where F(t) is the relaxation function of given property with β value being in the interval $0 < \beta \leq 1$. The non-exponentiality factor β represents the inverse proportionality to the width of distribution relaxation times. [11,66,67] The validity of this TNM model has been extensively explored during years, see examples in Ref. [69-72], where the good eligibility of this model in order to a description of structural relaxation processes was confirmed.

In regard to DSC data, the so-called reduced heat flow Φ^{red} (see Equation (24)) was estimated as a substitution of the relaxation function F(t) due to the requirement of the normalization of DSC data in the glass transition region, because the difference between the temperature dependences of heat capacity in the glassy and undercooled liquid regions occurs.

$$\Phi^{red} = \frac{\Phi(T) - \Phi_g(T)}{\Phi_l(T) - \Phi_g(T)} \tag{24}$$

where $\Phi(T)$ are the measured DSC data, $\Phi_g(T)$ and $\Phi_l(T)$ are the temperature dependences extrapolated from the glassy and undercooled liquid regions. [69]

2 Aims of Doctoral Dissertation

The doctoral thesis primarily pursues the detailed systematic study and characterization of crystallization behavior of tellurium-based chalcogenide glassy systems with respect to the kinetic processes and their kinetic description by means of commonly used kinetic models and state-of-art methodologies, the structural arrangements occurring in studied systems, and the appraisal of potential real-life applicability of these materials. Also the structural relaxation kinetics has to be described (rather as a side-note) due to the need of the completion of crystallization results for the next predictions of processability and stability of studied materials.

The crystallization process of tellurium-based glasses often shows a certain degree of complexity, which means that the individual crystallization peaks overlap, the beginning and the end of each single peak cannot be easily determined and the crystallization kinetic analysis cannot be properly performed. This issue is commonly solved by means of deconvolution procedure. It means that the set of experimental data are separated to particular components via the various methods of deconvolution. In the doctoral thesis, the two ways of deconvolution procedure were used, namely the kinetic deconvolution with usage of multivariate kinetic analysis (which belongs to the group of model-fitting methods) and the mathematic deconvolution, which is based on several mathematical functions, in case of this thesis, the Fraser-Suzuki function was used in particular with following kinetic analysis of individual crystallization processes.

The last area of interest of the doctoral thesis holds the potential practical usage of studied chalcogenide tellurium-based glassy systems. This issue is considered by means of glass stability criteria, which are the useful tools for this purpose. The typical commonly used glass-stability criteria (such as Hruby [28] criterion or the difference between the crystallization and glass transition temperatures) mostly provide a good information about material's glass-stability, but rather qualitative. [18,63-65] Regarding this limitation, the newly developed criteria for the evaluation of glass

stability are suggested [70], described and tested. These new-developed criteria come out from the possibility of the combination of results provided by DSC and TMA; due to the missing information from DSC about glass-softening processes, viscous flow effects and so on. These methods, with which the presented thesis works, belong to the thermo-analytic methods, which are based on an indirect observation of e.g. crystallization processes by means of certain macroscopic property (heat flow and sample deformation in case of the presented thesis) [15-20,72,73]. The opportunity to combine the results from DSC and TMA offers a certain benefit with regard to the assessment of glass stability of glassy materials.

More on above-mentioned aims and goals of the doctoral thesis will be discussed in following chapter. All studies presented in the doctoral thesis are published as the articles in impacted international journals.

3 Results and Discussion

3.1 Part I

As has been specified earlier, the doctoral thesis deals with the thermal, kinetic and structural characterization of tellurium-based chalcogenides glasses. It was mentioned that the Te-based glasses show a strong tendency towards crystallization. This problem may be solved e.g. by adding of various dopants into the tellurium matrix due to the stabilization of glassy system against devitrification [3-14]. The dopants used for the following studies in case of Ge-Te glasses were selenium, gallium and iodine; these dopants were added into Ge-Te matrix in various amounts along the investigated compositional lines due to the effort to uncover the most suitable composition in regard to potential practical usage. The next studied system, the As_2Se_3-As_2Te_3 glass, belongs also to Te-based glasses and was explored with various representations of As_2Te_3 part along the investigated compositional line. Thus, the systematic detailed study of thermal behavior of $Ge_{20}Se_xTe_{80-x}$ (x = 2; 4; 6; 8 %) [75-77], $Ge_{21}Se_xTe_{79-x}$ (x = 2; 4; 6; 8 %) [78], $(GeTe_4)_x(GaTe_3)_{100-x}$ (x = 40; 50; 60; 67; 75; 86; 100 %) [70,79-81], $Ge_{20}I_xTe_{80-x}$ (x = 2; 5; 8; 12; 15 %) [82,83] and $(As_2Se_3)_{100-x}(As_2Te_3)_x$ (x = 0; 17; 34; 50; 67; 84; 100 %) [84,85] chalcogenide systems was performed by means of DSC (primarily and for the kinetic analysis purposes), the experiments were carried out under non-isothermal conditions, which means that the monitored property (heat flow) was observed in dependence on temperature, and various sample forms (powders, bulks) were examined with regard to the predicative potential of the realized kinetic calculations.

The characterization of thermal behavior of investigated glassy systems may be done with usage of the simple scheme illustrated in Fig. 6. Firstly, the raw DSC curves are needed to be investigated with respect to a presence or an absence of expected thermal effects (e.g. glass transition, crystallization, melting), the nature of crystallization effect (e.g. single-peak/multiple-peak behavior) and its behavior under various experimental conditions (e.g. sample form, applied heating rate). Thereafter, the structural analysis of obtained crystallization products needs to be done due to their structural characterization (e.g. XRD, IR microscopy, Raman spectroscopy) and this step can help to identify the ongoing processes in the studied

materials. Afterwards, the kinetic analysis is carried out and the complete information about the given system is acquired with the combined knowledge about thermal, structural and kinetic properties.

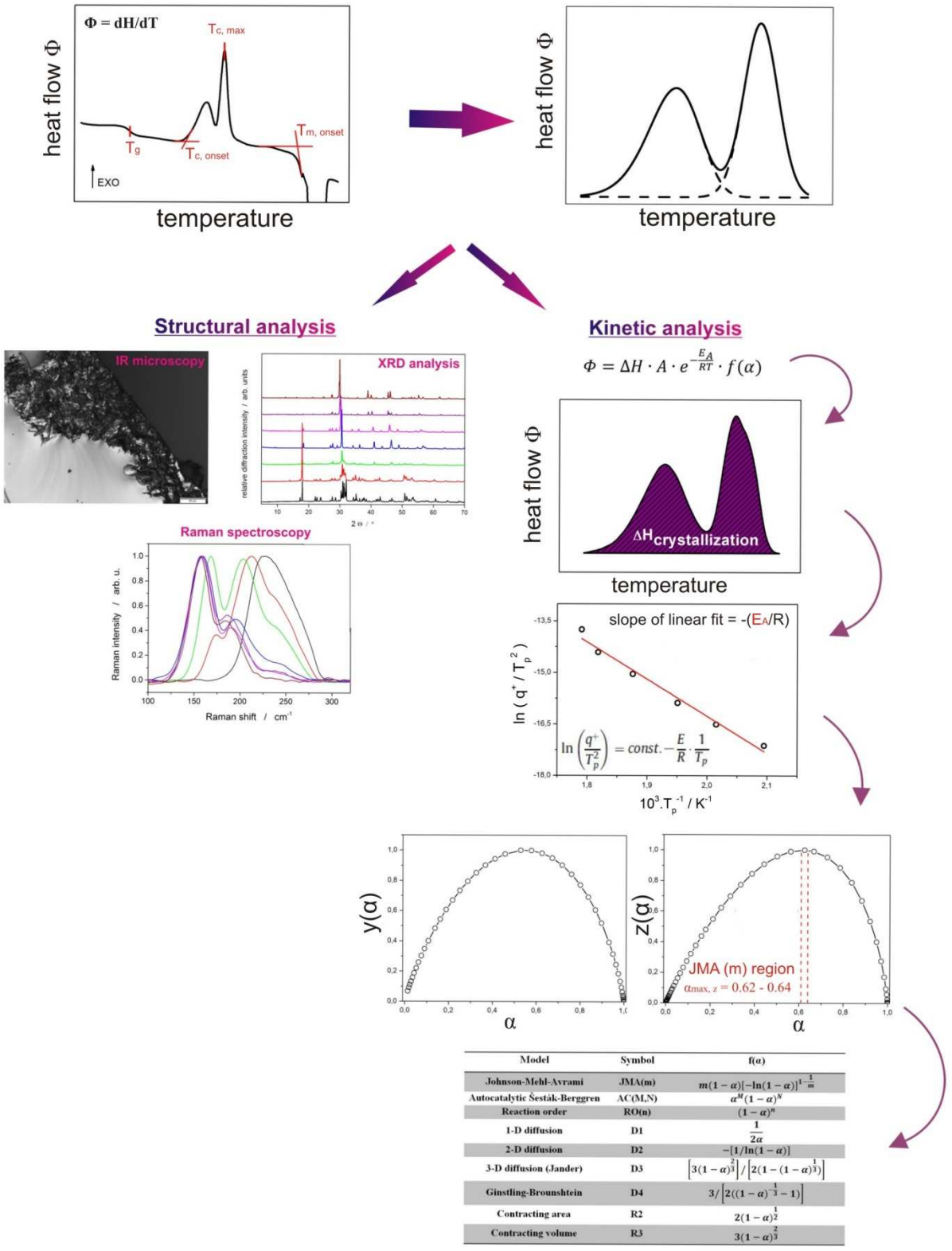

Model	Symbol	f(α)
Johnson-Mehl-Avrami	JMA(m)	$m(1-\alpha)[-\ln(1-\alpha)]^{1-\frac{1}{m}}$
Autocatalytic Šesták-Berggren	AC(M,N)	$\alpha^M(1-\alpha)^N$
Reaction order	RO(n)	$(1-\alpha)^n$
1-D diffusion	D1	$\frac{1}{2\alpha}$
2-D diffusion	D2	$-[1/\ln(1-\alpha)]$
3-D diffusion (Jander)	D3	$\left[3(1-\alpha)^{\frac{2}{3}}\right] / \left[2(1-(1-\alpha)^{\frac{1}{3}})\right]$
Ginstling-Brounshtein	D4	$3/\left[2((1-\alpha)^{-\frac{1}{3}}-1)\right]$
Contracting area	R2	$2(1-\alpha)^{\frac{1}{2}}$
Contracting volume	R3	$3(1-\alpha)^{\frac{2}{3}}$

Figure 6: The illustration of procedures used to characterization of thermokinetic behavior of investigated chalcogenide systems.

3.1.1 Ge-Se-Te system

As the first researched material for the doctoral thesis objective the selenium-doped $GeTe_4$ glass was selected, the thermal behavior of which was investigated along two selected compositional lines, namely the $Ge_{20}Se_xTe_{80-x}$ (x = 2; 4; 6; 8 %) [75-77] and $Ge_{21}Se_xTe_{79-x}$ (x = 2; 4; 6; 8 %) [78] glassy compositions. The amount of added selenium had to be held under 10 at. % due to its influence on the final width of transmittance window. In addition, the glassy composition with 10 at. % of Se is probably near to the non-mixing zone and on that account its thermal stability decreases [4,6,10,14,86-89].

The crystallization behavior of the studied systems is greatly influenced by the added amount of selenium into Ge-Te matrix, which is reflected in the separation of the primal surface tellurium precipitation from the subsequent volume-located GeTe and GeTe(Se) (phase contains all three elements) crystal growth (supported by XRD analysis). Also, the occurrence of selenium leads to inhibition of both crystallization mechanisms. Selenium integrates into GeTe network and, as well, into Te-chains; that can be the reason for the obvious separation of crystallization peaks with increasing amount of selenium in Ge-Te matrix.

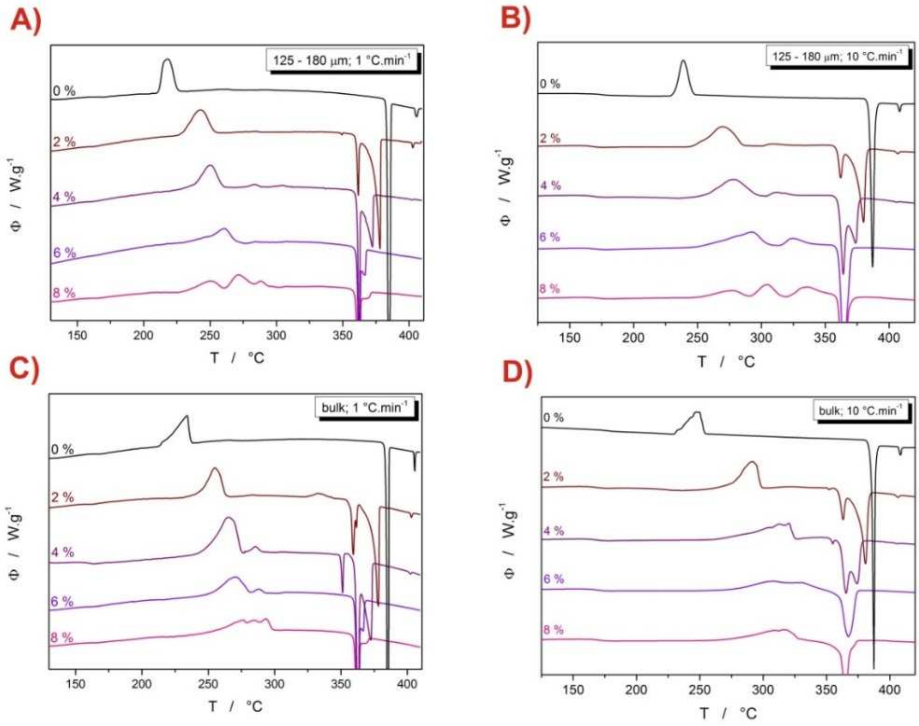

Figure 7: Example DSC curves obtained for applied heating rates 1 and 10 °C.min^{-1} and the 125-180 μm powders (graphs A and B) and bulk samples (graphs C and D) of the studied $Ge_{21}Se_xTe_{79-x}$ glasses. Each curve is marked according to the Se at. % content. Exothermic effects evolve in the "upwards" direction.

With using the Kissinger method [41] the apparent activation energy of crystallization was determined and the obtained E_A values can be found in Fig. 14A. As can be seen, the significant decrease in the E_A values representing the compositions with added selenium in comparison with pure $Ge_{21}Te_{79}$ system is observable. This change in E_A is caused by the first addition of selenium into pure GeTe matrix, which is accompanied by the change of the main crystal growth mechanism. While in case

of $GeTe_4$ glass, only the surface crystallization was found [90] and the accelerating influence of mechanically induced defects on the primary crystallization process was confirmed, the Se-doped glass shows the two types of crystallization mechanisms, namely the surface Te precipitation and some volume-located crystals form (see Fig. 8); the addition of Se leads to a change in crystallization mechanism. These findings are also in good correspondence with the study focused on the influence of the Se ↔ Te substitution on crystallization mechanisms [91], where it was also shown, that the smaller number of large crystallites occurs with the addition of Se into $GeTe_4$ matrix. These crystallites exhibit a three-dimensional growth.

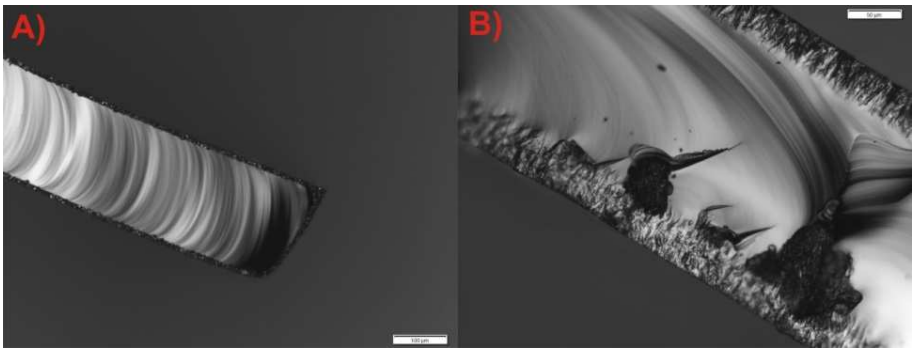

Figure 8: Selected infrared micrographs corresponding to the cross-section views of the partially DSC-crystallized pure $GeTe_4$ (A) and $Ge_{20}Se_2Te_{78}$ (B) materials.

The occurrence of two types of crystallization mechanisms was confirmed also by a huge IR microscopy study [92], which was also used, for the first time, to directly confirm the crystallization originating from the mechanically induced defects. The partially-crystallized (in DSC) samples were prepared; the selected grains were carefully cracked and observed by IR microscope. Each piece of tested grains contained a large number of small crystallites, the presence of which confirmed the predicated defects-based crystallization. Also a large number of fragments were on their surfaces covered by a crystalline layer.

It was found that the fine alteration in amount of Ge in Ge-Te matrix ($Ge_{20}Te_{80}$ – [75] vs. $Ge_{21}Te_{79}$ – [78]) has not been critical, has not had any marked influence on thermal behavior and the results have been mostly similar, thus allowing making the same conclusions and the crucial influence on thermal behavior of the Se-doped glasses has been caused by the added amount of selenium.

To conclude the problematics of crystallization kinetic behavior of studied Se-doped GeTe glass, it must be noted that this material follows the JMA/AC kinetics. The characteristic $z(\alpha)$ and $y(\alpha)$ functions were utilized in order to determine the appropriate kinetic model $f(\alpha)$. The appropriate kinetic model can then be chosen upon the value of degree of conversion α corresponding to the maximum of this function. As can be seen in Fig. 9A, the basic requirement of JMA (m) model ($\alpha_{max,\ z}$ equals to 0.62 – 0.64; this value is indicated by red dashed line in Fig. 9A) is fulfilled for most measurements performed at different heating rates and the most of kinetic data could be described by JMA (m) model, except the borderline experimental conditions (the lowest and the highest applied heating rates). In this case, the more flexible AC(M,N) model was used for description of the crystallization kinetics.

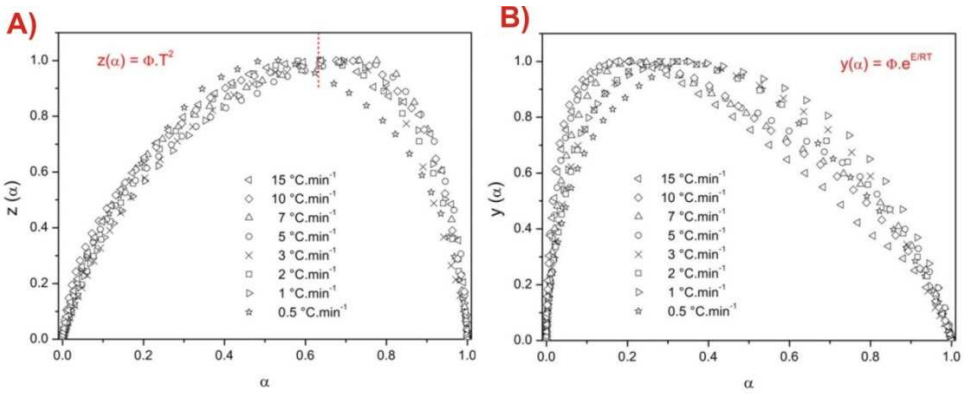

Figure 9: An illustration of set of characteristic functions z(α) (A) and y(α) (B) calculated for the set of crystallization DSC measurements performed for $Ge_{21}Se_4Te_{75}$.

The values of maxima of y(α) function (see Fig. 9B) serve for the determination of the parameters (m, M, N) of the previously found kinetic models (based on Equations 14, 16 and 17). The parameter m reflects the information about the dimensionality of formed crystallites. It was determined (based on the Eq. 14) that the crystallites formed as a 3-dimensional crystals under the lower heating rates, while as the applied heating rate increased, the crystal dimensionality decreased (to ~ 2) and the planar/surface crystals were formed. The change of crystal growth dimensionality occurs with increasing heating rate. Lastly, the value of preexponential factor A was determined ($A \sim 1.1 \cdot 10^{15}$) and the crystallization peaks could be described by the most suitable kinetic model.

The combination of dilatometric and calorimetric approaches used for the study of kinetic processes in $Ge_{20}Se_4Te_{76}$ glass is shown in [77]. The crystallization behavior was examined by means of DSC and TMA. The combination of these two techniques offers an interesting sight into ongoing processes in materials in further detail, because the DSC experiments do not give the appropriate information about processes connected with softening of glassy material and viscous flow effects, which play an important role in the overall crystallization process. Also these processes largely influence the stability of glassy materials and their potential usage. Due to these motives, the correlation between these two techniques was searched for and a good agreement was found. Therefore, the crystallization kinetics was described by usage of DSC and also by usage of TMA data, whereas regarding the TMA data the T_p value (corresponding to the maxima of crystallization DSC peak) was replaced by the T_{ic}. The initial crystallization temperature T_{ic} obtained from the crystallization TMA measurements corresponds to an intersection of extrapolations from the inflexion point and final stabilized sample height. As was shown in Refs. [96-98], the dependence of T_{ic} on temperature follows on the Arrhenian kinetic assumptions, thus this parameter can be used for the kinetic analysis of crystallization. The evaluated apparent activation energies of $Ge_{20}Se_4Te_{76}$ crystallization obtained from the DSC and TMA data were very close, which was fairly startling due to the fact, that the E_A values provided by TMA used to be higher than the E_A values provided by DSC, because the DSC measurements give values corresponding to the overall crystallization process, while the E_A values determined by means of TMA usually correspond to the initial state of crystallization process. This fact can be explained on the basis of significantly higher amount of crystallites, which is needed for

the formation of firm crystalline network and consequently for stopping the strong viscous flow in the $Ge_{20}Se_4Te_{76}$ glass.

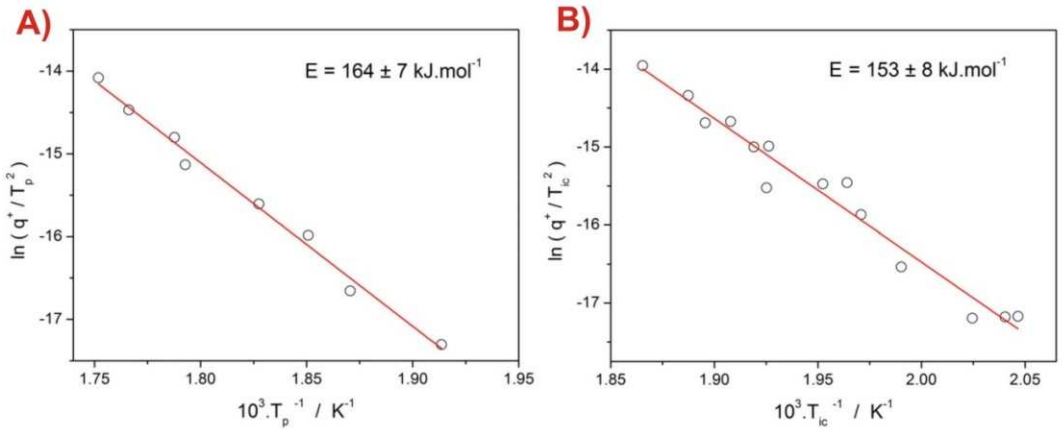

Figure 10: Kissinger plots constructed for the set of crystallization DSC (A) and TMA (B) measurements performed for the $Ge_{20}Te_{76}Se_4$ bulk glass.

3.1.2 Ge-Ga-Te system

The other promising materials for far-infrared optics applications can be the Ga-doped $GeTe_4$ glasses. The great advantage of choice of gallium as a dopant lies in the fact, that the presence of gallium in fully telluride matrix does not influence so much the width of transmittance window (can reach up to 28 μm [8]), therefore the Ga-doped $GeTe_4$ systems can introduce the good compromise between the thermal stability and optical properties of resulting glass. The doctoral thesis includes several studies [70,79-81] focused on a detailed characterization of thermal, structural and kinetic behavior of $(GeTe_4)_x(GaTe_3)_{100-x}$ (x = 40; 50; 60; 67; 75; 86; 100 %) chalcogenide systems due to the limited knowledge about the thermo-kinetic and structural properties of this system.

In Fig. 11A, the DSC curves obtained for $(GeTe_4)_x(GaTe_3)_{100-x}$ (x = 40; 50; 60; 67; 75; 86; 100 %) systems for chosen experimental conditions are displayed. The impact of the Ga addition is obvious, the uniform single peak representing the pure $GeTe_4$ splits into two crystallization sub-peaks, which can be best noticed for the powder fractions. The important observable fact is that the crystallization onset remains invariable. The relative invariability of crystallization onset with composition can be explained as the fact that low amounts of gallium is needed to the saturation of centers intended for Te precipitation. So, it can be stated that gallium functions not only as a stabilizing factor of GeTe network, but also influences the precipitation of tellurium by preferentially occupying the crystallization centers primarily intended for the tellurium precipitation. It is worthy of notice, that the evolution of the shape of melting peaks (see Fig. 11A) points out to the existence of eutectic (at ca. 357 °C); the exact eutectic composition appears to be close to $(GeTe_4)_{67}(GaTe_3)_{33}$.

The first and very important difference in the crystallization mechanism and role of gallium (as dopant) in $GeTe_4$ matrix compared to Se-doped glasses emerges from the findings based on XRD analysis to which the partially-crystallized (heated to the maximum of the first peak) selected compositions (rich in gallium) were

subjected. The presence of Ga_2Te_5 phase was confirmed already during this first crystallization peak (besides the Te phase), and this is completely different behavior in contrary to previously mentioned Ge-Se-Te [75-78,90,91] and afterwards discussed Ge-I-Te [82,83] systems, where the crystal growth of the GeSeTe and GeI phases is centered in the second crystallization mechanism, while in the partially-crystallized products (heated to the maximum of the first peak) only the hexagonal tellurium was present. This phenomenon can be explained on the basis of the previous structural study [96], that Ga atoms do not incorporate into the GeTe network and bond only to tellurium; as the Te precipitation begins, the Ga_2Te_5 phase forms too. These conclusions can be supported also by the results from IR microscopy (see Fig. 12A), where lower number of nuclei (for the higher amounts of Ga) can be seen in contrary to the pure surface growth.

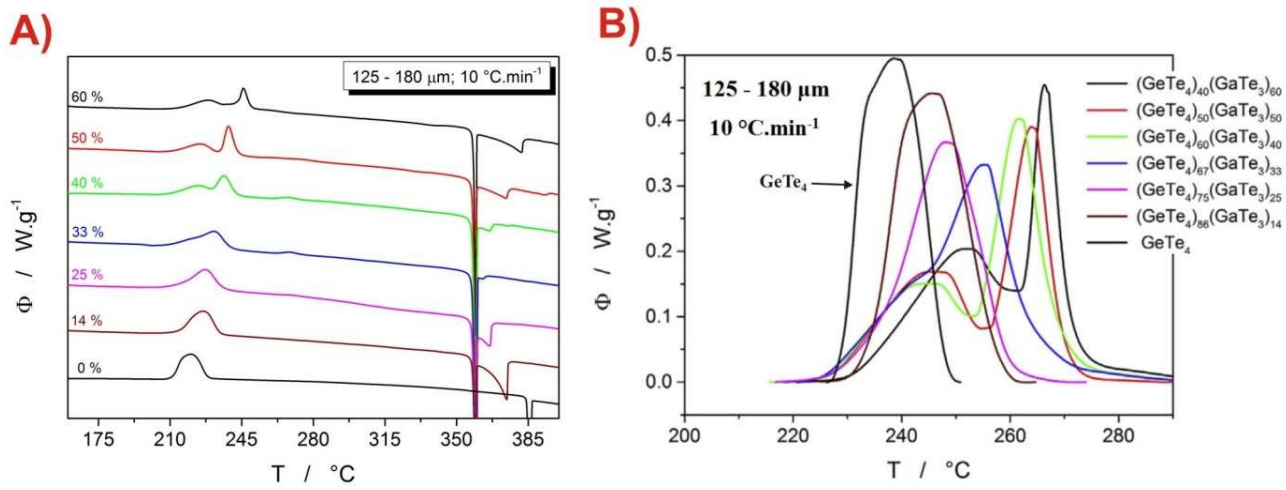

Figure 11: A) Example DSC curves obtained for applied heating rate 10°C.min^{-1} and the 125-180 µm powders of the studied $(GeTe_4)_x(GaTe_3)_{100-x}$ glasses. Each curve is marked according to the $GaTe_3$ at. % content. Exothermic effects evolve in the "upwards" direction.

B) Zoomed crystallization effects obtained for 125 - 180 µm powders heated at 10 °C.min^{-1}.

The Raman spectroscopy provided the information about structural arrangements in $(GeTe_4)_x(GaTe_3)_{100-x}$ systems. The impact of gallium on structural arrangements in Ge-Ga-Te system could not be assigned so simply. The illustrated Raman spectra in Fig. 12B denote that the present Ga content in $GeTe_4$ matrix induces the partial segregation of tellurium, which manifests as a larger signal corresponding to the Te chains (label C: 140 cm^{-1}). The presence of Ga content in $GeTe_4$ matrix probably leads to some strengthening of the $GeTe_4$ network, which manifests as a higher signal of the edge-shared tetrahedra (label D: 154 cm^{-1}). The most pronounced peak (label B: 125 cm^{-1}) was found to be representing the symmetric stretching mode of corner-sharing Te-rich $GeTe_4 - {}_nGe_n$ (n = 0, 1, 2) tetrahedra and the subtle peak (label A: 106 cm^{-1}) was found to be corresponding to the corner-sharing GeTe4 (n = 0) tetrahedral. [97-103]

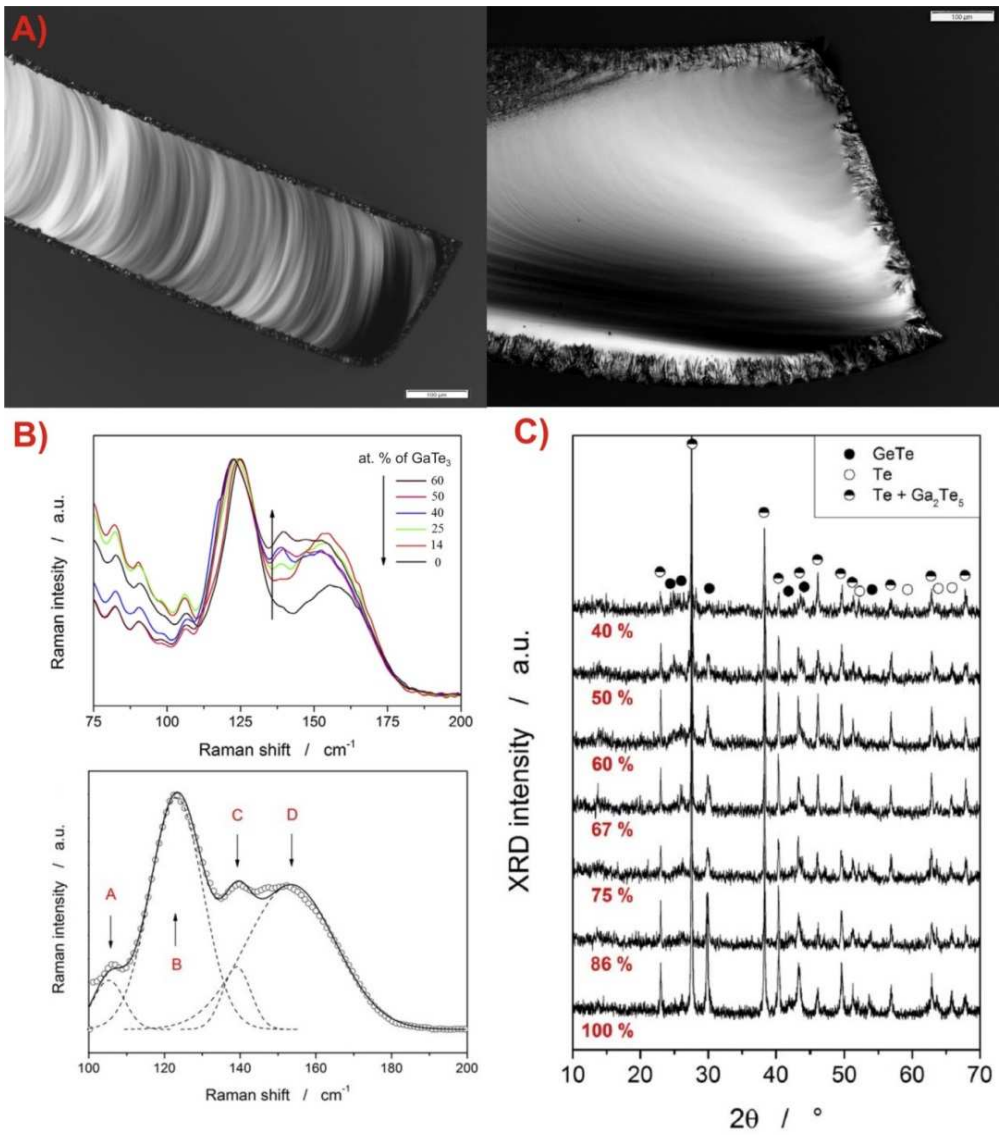

Figure 12: A) Infrared micrographs corresponding to the cross-section views of the partially DSC-crystallized pure $GeTe_4$ (the left-side micrograph) and $(GeTe_4)_{60}(GaTe_3)_{40}$ (the right-side micrograph) materials.

B) Raman spectra obtained for all investigated $(GeTe_4)_x(GaTe_3)_{100-x}$ glassy compositions (top) and Raman spectrum of chosen middle-positioned $(GeTe_4)_{50}(GaTe_3)_{50}$ glassy composition (below); dashed lines corresponding to the deconvoluted Gauss profile peaks, solid line corresponding to the overall fit, the circles corresponding to the experimental DSC data.

C) XRD records of crystallized $(GeTe_4)_x(GaTe_3)_{100-x}$ materials.

The multivariate kinetics analysis (MKA) was applied on DSC data to do the complete enumeration of the universal kinetic DSC equation (Eq. 7) for each dataset in order to describe the complex crystallization processes. The MKA optimization offered the combination of two independent crystallization sub-processes were found (based on the best correlation coefficient) to be following the JMA (m) and AC(M,N) kinetics. The JMA (m) model describes well the first (low-temperature) crystallization process, the AC(M,N) describes the second (high-temperature) crystallization process. The first process corresponds to the Te-precipitation and formation of hexagonal Ga_2Te_5 phase; the following second process represents the formation of rhombohedral GeTe and remaining Ga_2Te_5 phase. Naturally,

the MKA method provides values of all of involved kinetic parameters; for example see Fig. 14A. In Fig 14A, the estimated E_A values for bulk samples can be seen (the chosen E_A values corresponding to the dominant crystallization process). The relative consistent trend is observable, which plays an important role in e.g. glass-ceramics or infrared optics application areas, where the crystal growth needs to be controlled. The studies of crystallization kinetics of these systems in dependence on particle size were performed due to the confirmation of the influence of mechanically induced defects on crystallization behavior. It was found in [79-81] that the presence of mechanically induced defects amplifies the initial precipitation of Te and the first formation of Ga_2Te_5 phase (the magnitude of the first crystallization peak increases) with increasing $GaTe_3$ content and decreasing particle size. The study included in [80,81], focused on the effect of powder coarseness on crystallization kinetics of $Ge_{11}Ga_{11}Te_{78}$ glass (middle-positioned composition inside the studied pseudo-binary line), briefly supports these findings. The values of apparent activation energy were found to have a descending character with particle size for both sub-processes, which also points out on the growth from mechanically induced defects.

The $Ge_{11}Ga_{11}Te_{78}$ glass was also subjected to the combined thermal analysis [81], which was performed by means of DSC and TMA as for the case of Se-doped glasses, the same presumptions were approved. The results from MKA analysis were in a perfect agreement with those from TMA, only the relatively large errors associated with the evaluations of e.g. E_A from TMA measurements can be observed. This effect is probably caused by the worse reproducibility of determination of initial crystallization temperature, however the similar trend occurs. The results from thermal, structural and kinetic study of this glassy composition correlate very well with those quoted above.

3.1.3 Ge-I-Te

The doping of $GeTe_4$ glass by iodine introduces the third (and last option presented in the doctoral thesis) possible way how to stabilize the fully telluride matrix against crystallization and improve the thermal properties of this glassy material with respect to the potential applicability in area of any practical usage. The function of iodine as stabilizing factor lies firstly in its terminating role in the three-dimensional GeTe network, and secondly, the iodine atoms are capable to trap the electrons from tellurium. [44,46,47,89,104-108]

The results originating from the detailed study dealing with the thermal and structural characterization of the $Ge_{20}I_xTe_{80-x}$ (x = 2; 5; 8; 12; 15 %) system, included in [82,83], will be introduced. The crystallization process shows a certain degree of complexity (as for the Se- and Ga-doped systems), the occurring crystallization mechanisms overlap or compete against each other. The structural information achieved by means of XRD analysis revealed that the hexagonal tellurium, rhombohedral GeTe and minor amounts of cubic GeI_4 form during the crystallization process in case of all investigated compositions. The Raman spectroscopy analysis (Fig. 13B) was applied on freshly fractured bulk glasses and DSC-crystallized powders and structural units occurring in investigated system were identified. The impact of increasing amount of iodine in glassy matrix manifested probably in decreasing

trend of intensity of vibrations of edge-sharing $GeTe_4$ (or Ge-rich) tetrahedra or vibrations of short, amorphous, distorted tellurium chains [97-103].

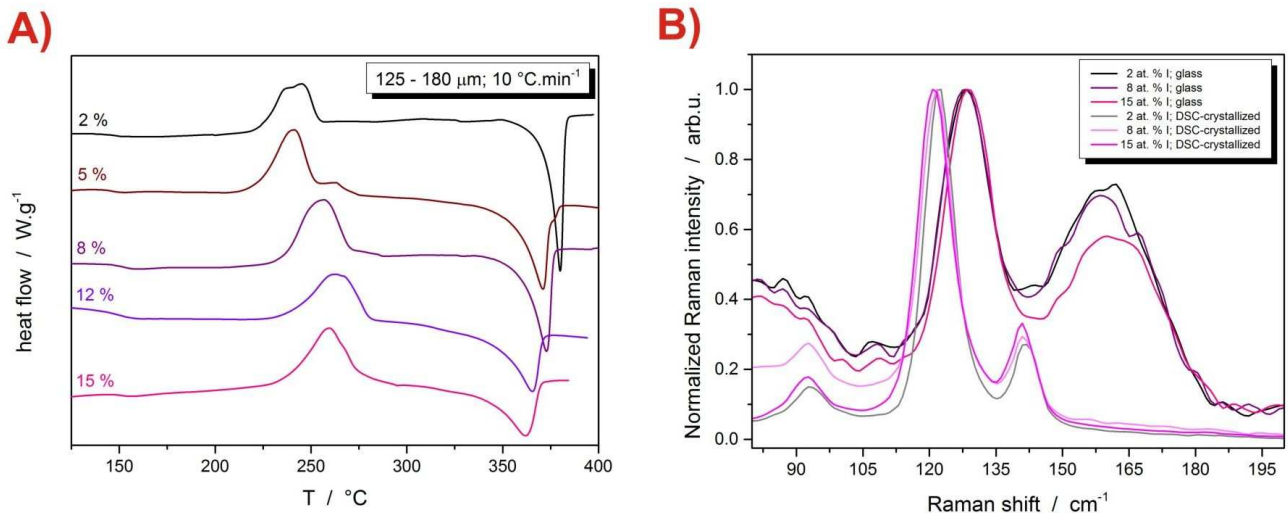

Figure 13: A) Example DSC curves obtained for applied heating rate 10°C.min^{-1} and the 125-180 μm powders of the studied $Ge_{20}I_xTe_{80-x}$ glasses. Each curve is marked according to the I at. % content. Exothermic effects evolve in the "upwards" direction.
B) Raman spectra of the selected glassy and DSC-crystallized $Ge_{20}Te_{80-x}I_x$ materials.

The typical kinetic behavior of crystallization process was observed, which means that the shift of crystallization to higher temperatures with higher heating rates and increasing particle size occurs. After standard mathematic deconvolution procedure (more about this method in the following chapter) the dominant volume-located crystal growth in case of bulk samples was exposed (as was expected). In case of powdered samples, the surface and volume crystal growth appeared to be comparable. The subsequent kinetic analysis was realized by the determination of all parameters of the universal DSC kinetic equation (Eq. 7). It was found, that the E_A values were significantly influenced by experimental conditions and any trend cannot be assigned (see Fig. 14A). This indicates a large variability of initial phase of crystallization with applied experimental conditions and accelerating impact of the presence of mechanically induced defects. The flexible AC(M,N) model was found as the best choice in order to kinetic characterization of the crystallization DSC data.

3.1.4 The structural relaxation behavior of doped Ge-Te systems

In the presented studies [70,75-78,81-83] the relaxation behavior of doped $GeTe_4$ glasses was characterized by means of relaxation kinetics. This is a valuable tool how to complete the thermal, kinetic and structural knowledge about investigated systems. However, in the doctoral thesis, the description of the relaxation behavior is not a key topic and serves rather as a complementary subject to the thermal (mainly crystallization) and structural assessments of the inquired chalcogenide systems. The relaxation kinetic processes in the given systems were described by using the TNM [11,66,67] model. This phenomenological model belongs to the commonly

used ways how to reveal the relaxation behavior of the various materials. Its basis and mathematic description was introduced above in Chapter 1.4.4, where this model was expressed by the set of mathematic equations (Eqs. 22 and 23). The relaxation behavior can be characterized using the parameter called the apparent activation energy of structural relaxation Δh^*, the evolution of which with various studied composition can be found in Fig. 14B. As can be seen, the initial addition of selenium slightly contributes to a decrease of the Δh^* values in case of the Se-doped $GeTe_4$ glass, which can indicate the coincidental incorporation of selenium into the $GeTe_{4-n}Ge_n$ tetrahedra. These processes probably correspond to the corner-/edge-shared tetrahedra ratio change, which means that the small amount of GeTe bonds would have to be broken to the change of conformation will be reached. It was pointed out [77], that the main portion of relaxation movements is carried by the $GeTe_4$ tetrahedra. These conclusions were supported by data from Raman spectroscopy and can be summarized as follows. The addition of selenium into GeTe matrix does not influence the position of T_g so much and the main portion of relaxation movements is carried by the $GeTe_4$ tetrahedra.

As was concluded in [70,81], the Ga atoms connects with the Te electronic lone pairs and do not interact with GeTe covalent network. That is a great difference as distinct from the previously reported results representing the Se-doped $GeTe_4$ glasses [75-78], where it was also established that the main portion of relaxation movements is undertaken by $GeTe_4$ tetrahedra. In contrary, in the case of Ga-doped $GeTe_4$ systems, the next dissimilarity arises, namely the presence of Ga-Te units influences the processes of relaxation movements in Ga-doped $GeTe_4$ glasses. It was found, that the Ga-Te units function as somehow diluting elements of the Ge-Te tetrahedral network, which leads to formation of small, partially sequestered $GeTe_4$ tetrahedral groups. These groups are separated by Te-chains and dimmers terminated by Ga. The decrease of available relaxation movements ensues from this dilution effect of Ga.

On the basis of structural relaxation study of $Ge_{20}I_xTe_{80-x}$ (x = 2; 5; 8; 12; 15 %) system [82,83] it was found that the iodine solely connects with germanium, therefore the structure is formed by the $GeTe_4$ and $GeTe_{4-x}I_x$ tetrahedra, which are linked by Te-Te bonds, that implies the iodine atom terminates the tetrahedral interconnections. This can be the explanation of lower values of Δh^* due to the less interconnection of matrix, which results in a lower amount of bonds needing to be transformed. In consequence of these effects of iodine on $GeTe_4$ matrix, the lower interconnectivity in glassy matrix is present (in comparison with pure $GeTe_4$) and in this case perhaps the larger structural units have to be moved to spread the relaxation movement. With respect to results from Raman spectroscopy, which do not indicate any major differences between the low I-doping (2 at. % of I) and higher I-doping (8 at. % of I), can be supposed that the surplus Ge is more capable to bond with iodine (forming the GeI_4 tetrahedra; the addition of iodine was at the expense of tellurium) and the terminating role of iodine is therefore narrowed. Also, a part of iodine appeared to be not covalently bonded in the Ge-Te-(I) matrix. The spontaneous condensation on the walls of vessels, in which the prepared glassy or crystallized samples were stored, occurred. However, the experimental characteristics (DSC records, Raman spectra) did not change after 3 months of storage.

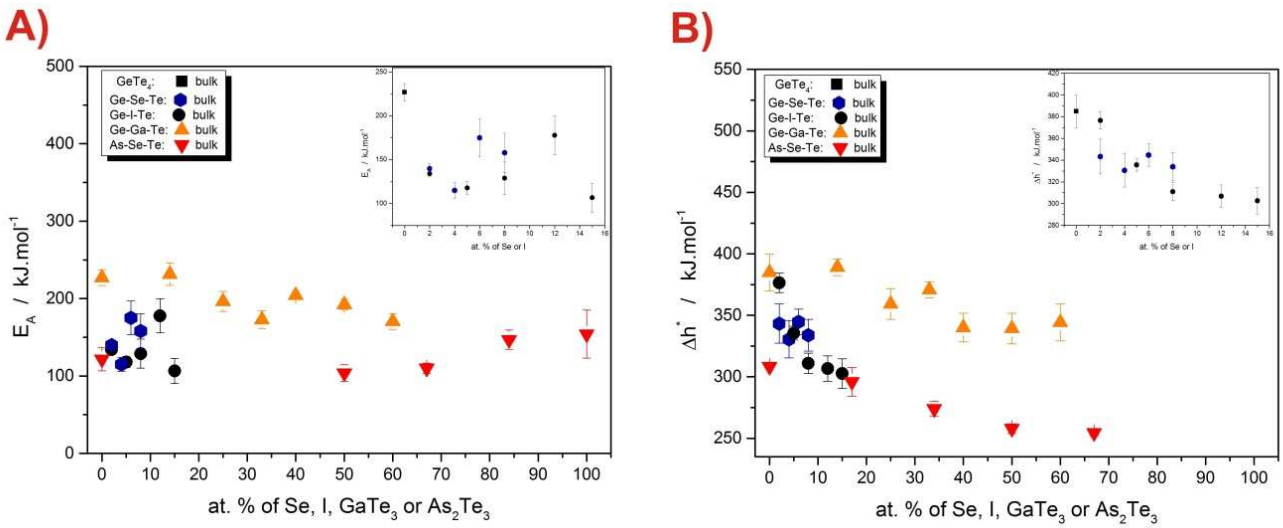

Figure 14: Compositional dependence of crystallization (A) and relaxation (B) activation energies for all investigated systems in form of bulk samples; the inset illustrates the zoomed area corresponding to the compositions with 0 - 15 at. % Se or I.

3.1.5 As-Se-Te system

An alternative to the investigated doped-$GeTe_4$ glasses is the As-Se-Te glass, where the As-Se content is added to As-Te fully telluride matrix in order to improve the thermal properties. It is believed, that As-Se-Te glasses can be comparable with doped-$GeTe_4$ glasses and the thorough knowledge of crystallization, relaxation and structural behavior is crucial for the next processing of glassy material. The As_2Se_3 binary system is well-known as an excellent glass-former and its addition to As_2Te_3 results in great improvement of thermal properties of glass. [3,7,9,12,44,87-89] Therefore, for the first time, thermal and structural behavior of As-Se-Te glasses was investigated in detail in the present doctoral thesis.

The doctoral thesis deals with the thermo-structural characterization of $(As_2Se_3)_{100-x}(As_2Te_3)_x$ glasses along the whole compositional line [84] and with the thermal characterization of middle-positioned composition on the promising pseudo-binary line, namely the $(As_2Se_3)_{50}(As_2Te_3)_{50}$ system [85].

Typically, the XRD analysis was used for identification of created crystallization products and some complications with a definition of structure arose. It was found, that monoclinic As_2Te_3 and As_2Se_3 units form (the pure As_2Te_3 and As_2Se_3 compositions), also the neighboring compositions (with 17 and 84 at. % of As_2Te_3) manifest the similar crystalline phases (only with slight shift of diffraction lines). However, the intermediate compositions (34, 50, 67 at. % of As_2Te_3) showed that completely different crystalline phases emerge. With using the temperature-resolved XRD analysis it was revealed that at the beginning of crystallization process the cubic $As_{50}Se_{25}Te_{25}$ forms, however the re-crystallization of this phase into more stable monoclinic As-Se-Te probably took place very quickly.

From the results provided by Raman spectroscopy it could be read that the significant changes in structure with addition of tellurium manifest up to 50 at. % of As_2Te_3. Above this percentage, the representation of As_2Te_3 the structure changes minimally with addition of tellurium. The assignment of structural arrangements in

investigated glassy systems can be carried out on the basis of deconvolution of obtained Raman spectra (via Gauss function).

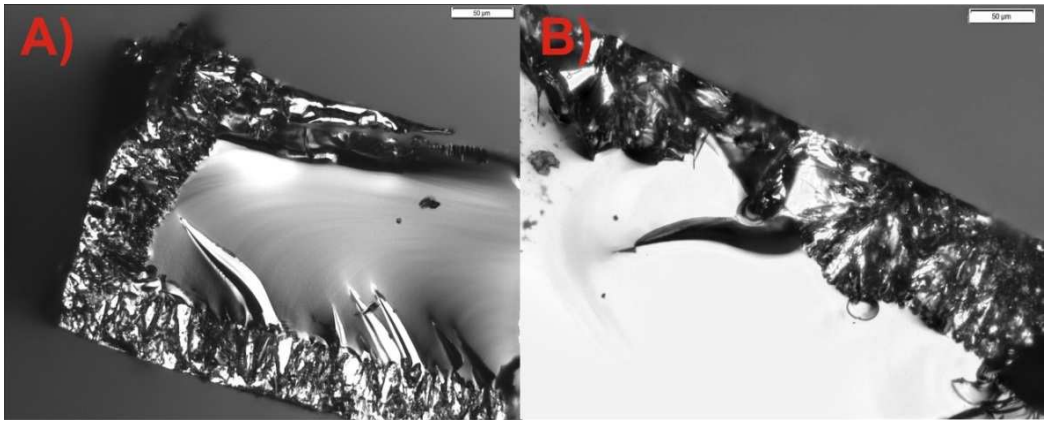

Figure 15: Infrared micrographs corresponding to the cross-section views of the partially DSC-crystallized As_2Te_3 (A) and $(As_2Se_3)_{50}(As_2Te_3)_{50}$ (B) materials.

The IR microscopy analysis was performed in order to better recognize the crystallization mechanisms and morphology of formed crystalline phases. The presence of two morphologically different crystallites was observed. The spherulites, which form predominantly in case of compositions with increasing amount of As_2Se_3, and needle-shapes crystals characteristic for As_2Te_3-rich compositions. All the samples crystallize on surface with subsequent inward crystal growth. This type of crystallization was also observed for previously studied $GeTe_4$ glasses and it can be supposed that the presence of surface crystallization mechanism is associated with rising amount of tellurium in the structure.

For the 50/50 composition [85], the structural study (XRD analysis, Raman spectroscopy, IR microscopy) proved the complicated structural arrangement. The physical dispositions of As_2Se_3 and As_2Te_3 phases permit to interchange each other in the structure. The $As_2Se_3 \leftrightarrow As_2Te_3$ substitution exists. The difficulties of unambiguous determination of crystallization morphology occurring in $(As_2Se_3)_{100-x}(As_2Te_3)_x$ system produce also the random incorporation of Te in the structure. No strict structural morphology exists. This can explain the observed complexity of the crystallization processes.

The two crystallization sub-processes correspond to the development of morphologically different crystalline phases – the needle-shaped vs. spherulitic crystallites. The crystallization complexity occurs also in case of pure As_2Te_3, it can then correspond to the initial formation of cubic AsTe phase (the first peak), which recrystallizes into stable monoclinic As_2Te_3, and the second crystallization process then corresponds to the recrystallization of remaining cubic AsTe phase. The large disinclination to crystallization was marked for As_2Se_3-rich side of studied compositional line; only the composition containing 34 at. % of As_2Te_3 slightly crystallizes under certain conditions (low heating rate, powdered sample). This composition seems to be very close to the eutectic point (see the complex shape and changes of melting peak profile with composition). On the basis of the possible presence of eutectic alloy (between 34 and 50 at. % of As_2Te_3) the extensive stability against crystallization can be clarified.

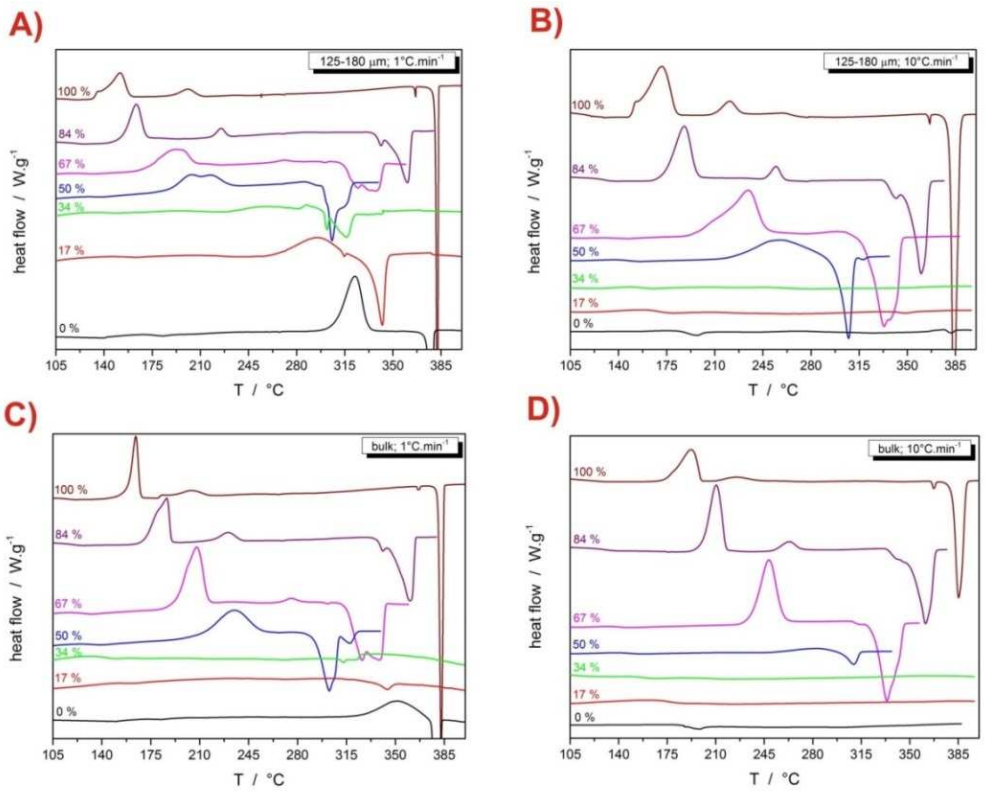

Figure 16: Example DSC curves obtained for applied heating rates 1 and 10°C.min^{-1} and the 125-180 μm powders (graphs A and B) and bulk samples (graphs C and D) of the studied $(As_2Se_3)_{100-x}(As_2Te_3)_x$ glasses. Each curve is marked according to the As_2Te_3 at. % content. Exothermic effects evolve in the "upwards" direction.

In regard to the choice of the suitable kinetic model, the JMA (m) and AC(M,N) models were tested. As is apparent from Fig. 17, the only one (the coarsest one) of powder fractions is close to the JMA(m) model usability condition. For the best description of crystallization kinetics of $(As_2Se_3)_{100-x}(As_2Te_3)_x$ (x = 0; 17; 34; 50; 67; 84; 100 %) system the AC(M,N) model was selected (also due to its flexibility to experimental data). The significant influence of experimental conditions (sample form, applied heating rate) on crystallization kinetics was found, thus the individual steps of potential processing of this glassy system must be critically controlled.

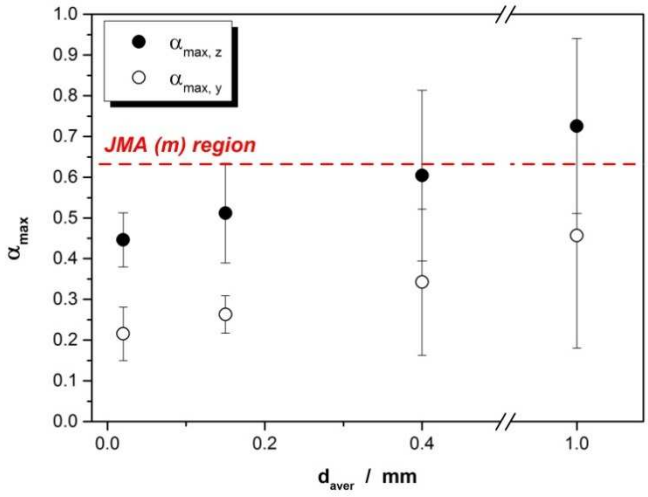

Figure 17: The dependence of the maxima of characteristic functions y(α), z(α) on the averaged particle size representing the $(As_2Se_3)_{50}(As_2Te_3)_{50}$ system.

The relaxation processes in $(As_2Se_3)_{100-x}(As_2Te_3)_x$ (x = 0; 17; 34; 50; 67; 84; 100 %) glass were described in terms of TNM model. It must be noticed that for compositions containing more than 67 at. % of As_2Te_3 the signals were very weak and scattered, so that the acquisition of reliable information was not possible. The decreasing trend in values of apparent activation energy of structural relaxation Δh^* (see Fig. 14B) of As_2Se_3-rich part of investigated compositional line appeared to be bound towards the Δh^* value equal to 258 $kJ.mol^{-1}$ (in the As_2Te_3-rich part). The significant decrease in T_g values was also marked. As was said, the Raman spectra revealed the minor changes in structure occurring in compositions containing more than 50 at. % of As_2Te_3 with the further addition of As_2Te_3. The rest of selenium was found to be primarily bound in the combined $AsTe(Se)_3$ pyramids and only part of selenium goes to form the pure $AsSe_3$ pyramids, which is in good correspondence with the compositional evolution of Δh^* values and T_g. As the As_2Se_3 content decreases, the Δh^* values also decrease due to the weaker As-Te bonds in contrary to As-Se bonds in $AsSe_3$ pyramids, therefore the energy needed to structural arrangements is also smaller. The replacement of fully selenide pyramidal units ($AsSe_3$) by mixed $AsTe(Se)_3$ pyramids causes the cessation of the Δh^* value decrease at lower As_2Se_3 amounts due to the dependence of these pyramids on distortion of the weaker As-Te bonds. The energy of relaxation movements does not depend on selenium content.

3.2 Part II

In this section, the complex kinetics manifesting in case of crystallization of glasses and the ways how to solve this phenomenon will be introduced. As was said, the crystallization process of tellurium-based glasses often shows a certain degree of complexity, which means that the individual crystallization peaks overlap and at least two kinetic mechanisms proceed simultaneously. The most of solid-state processes are complex, the revelation lies in an application of different experimental conditions (e.g. heating rate). In practice, the thermoanalytical records can show either only partial overlap or a pseudo-single peak behavior.

In general, there are three approaches how to treat such complex kinetics. The first approach offers such a way of the methods suggested primarily for single-process kinetic analysis applied on whole complex data-set and the following interpretation of changes and distortions of the obtained data. Usage of isoconversional methods for determination of activation energy (e.g. KAS [41] method) can serve as an example. The second approach uses the procedures of mathematic deconvolution of the complex kinetic signal using some suitable mathematic functions. After that, each set of these peaks is separately evaluated by means of normal single-process analysis. As a suitable mathematic function was found the Fraser-Suzuki (FS) [62-65] function, which was thoroughly tested in the past and it was confirmed that the FS function can describe all kinetics readily occurring for the solid-state reactions. [62-65] The FS function is expressed via the Eq. (21) and offers a reliable description of crystallization complexity observed for non-isothermal data. In case of isothermally obtained data, the Avrami [48-50,109] dogma can serve for the isothermally obtained complex data. The third approach includes a full reaction scheme containing all

the kinetic equations and their determination proceeds by means of non-linear optimization for all involved sub-processes simultaneously. This is called kinetic deconvolution. The multivariate kinetic analysis (MKA) was found as a the most suitable procedure, it represents a curve-fitting routine in terms of full-scale complex kinetics and model-free results (E_A and A) obtained for overall signal are used as input parameters [45,55-59]. All these methodologies are established and work very well.

However, if the kinetic behavior of the involved sub-processes changes with the experimental conditions (temperature, heating rate), these phenomena can be presented by the change of intensity of involved sub-processes likewise the increase or decrease of the enthalpy ΔH in case of DSC measurements; or kinetic mechanism can change for the given sub-process or simply the activation energy of each sub-process can be temperature or heating rate dependent. The above-mentioned facts are summarized in [110], which is focused on solution of crystallization kinetics complexity of glassy materials. It was found that the change of crystallization kinetics of particular sub-processes with temperature or heating rate is real and can occur for complex glassy matrices as well as for single-element glasses (chalcogenide Ge-Ga-Te glass vs. selenium glass vs. vanadium-doped ZrO_2 catalyst vs. $Y_3Al_5O_{12}$ microspheres). The kinetics variability can be often only matter of the extent of applied experimental conditions. The conclusions resulting from [110] can be interpreted as follows. The crystallization of the germanium-gallium-tellurium far-infrared glass can serve as the example of the examined systems. After the multivariate kinetic analysis was applied on tested data, it was found, that the kinetic parameters change in dependence on the range of considered heating rates, which means that the kinetics depends on heating rate.

Table 2: The summary of kinetic parameters obtained via MKA for the $(GeTe_4)_{50}(GaTe_3)_{50}$ material (different sets with given ranges of applied heating rates). The errors associated with these evaluations were lower than 0.02 for A, 0.2 for E_A, 0.02 for m_{JMA} and M and 0.01 for N parameter.

q^+ range / parameters	0.5 - 2 °C.min^{-1}	7 - 30 °C.min^{-1}	0.5 - 30 °C.min^{-1}
log (A_1 / s^{-1})	18.06	17.00	18.60
$E_{A\,1}$, kJ.mol^{-1}	199.45	188.02	203.86
m_{JMA}	1.68	1.49	1.44
log (A_2 / s^{-1})	22.32	17.55	17.70
$E_{A\,2}$, kJ.mol^{-1}	237.42	192.52	194.22
N	1.55	1.20	1.18
M	0.92	0.83	0.81

The both deconvolution procedures (mathematic and kinetic) provided suitable and consistent results (see [70,75,76,78-85,90,91,95,110]). The examples of selected deconvoluted DSC curves representing all of investigated systems (Se-, Ga-, I-doped $GeTe_4$ and As-Se-Te glasses), which the doctoral thesis includes, are illustrated

in Fig. 18. The number of curves, on which the deconvolution procedures were applied (within the framework on the doctoral thesis) exceeds one thousand, excepting the Ge-Ga-Te system (MKA was applied), the mathematic deconvolution was applied on all of investigated data. The usage of MKA method is easy and fast and introduces an effective method at distinguishing of subtle changes and trends in evolution of kinetic parameters. However, this method requires the more-or-less constant values of E_A across the whole explored range of experimental conditions. This condition was fulfilled only for the explored $(GeTe_4)_x(GaTe_3)_{100-x}$ (x = 40; 50; 60; 67; 75; 86; 100 %) system [70,79-81]. In contrary, the mathematic deconvolution procedure, which is followed by kinetic analysis of each of determined single processes, can be comparatively difficult and time consuming and was needed to be used in most case of studied systems [75,76,78,82-85,90,91,95,110]. Nevertheless, this method represents a valuable tool for deconvolution purposes, when the kinetic deconvolution cannot be performed - for example in case, when data exhibit great changes of E_A values with experimental conditions. If the potential mutual inter-dependences of the fundamental sub-processes exist, the mathematic deconvolution is not able to properly account for this phenomenon (in comparison with MKA). For the physically meaningful interpretations there is only the way of the deconvolution of each separate curve followed by displaying various trends in dependence on the temperature or heating rate ranges.

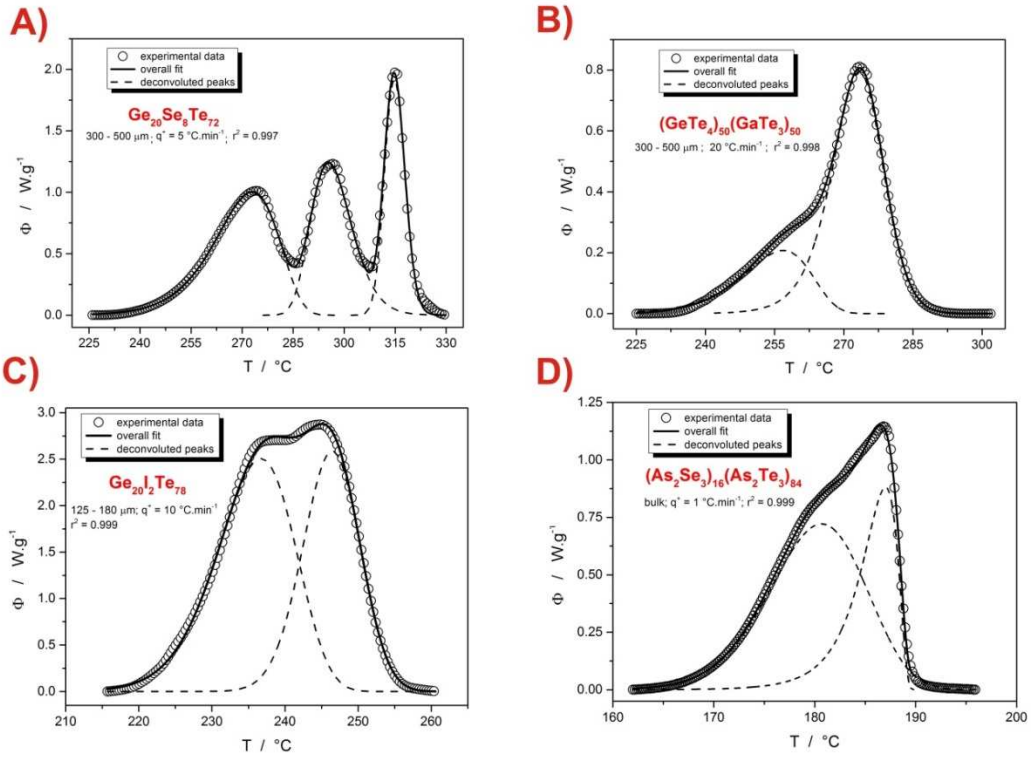

Figure 18: The examples of deconvoluted DSC curves representing the studied systems: A) $Ge_{20}Se_8Te_{72}$ system; B) $(GeTe_4)_{50}(GaTe_3)_{50}$ system; C) $Ge_{20}I_2Te_{78}$ system; D) $(As_2Se_3)_{16}(As_2Te_3)_{84}$ system.

The main purpose of this branch of the doctoral thesis was to draw an attention to this problematic and, hopefully, start off a research leading to some advancements or at least some activity regarding this issue.

3.3 Part III

The third section of the doctoral thesis will be focused on detailed characterization of thermal behavior of investigated glassy systems with regard to the assessment of glass ability and glass stability of the examined materials. This field of the characterization of glassy matters belongs to a very important area due to the appraisal of the potential usability of studied chalcogenide tellurium-based glassy systems in far-IR optics or glass-ceramics application areas. The various well-known glass-stability (GS) criteria are used for the consideration, whether the given material is able to form a stable glass. It has been pointed out above that the most suitable criterion (for chalcogenide materials) was found to be the Hruby criterion (see Ref. [34]), which unfortunately strongly depends on experimental conditions. The thermal stability of glassy systems can be considered also by using the so-called ΔT criterion ($\Delta T = T_c - T_g$) [8-10], which takes into account only the difference between the glass transition temperature T_g and the crystallization temperature T_c. However, this temperature difference has still remained crucial, the wider the difference $T_c - T_g$, the more stable the glass is. Nonetheless, the mentioned GS criteria work only with the characteristic temperatures and do not take into account the other facts, which fundamentally influence the resulting thermal stability of glass. Therefore, a new approach has been recently suggested [70]. The combination of crystallization temperature value (obtained from DSC crystallization measurements) and the information about glass-softening and viscous flow effects (obtained from TMA crystallization measurements) is applied. The glass-softening and viscous flow effects become more apparent and important in the crucial temperature region between the glass transition temperature and crystallization.

The direct correlation of thermo-kinetic and thermo-mechanical properties of Se- and Ga-doped GeTe systems is one of the contents of the doctoral thesis [70,77,78,81]. The Papers deal with the combined DSC and TMA study, which can provide the information about the true nature of the crystal growth process limiting the fiber-drawing procedures. The emphasis is put on getting as much information as possible from the combined DSC and TMA measurements, and also on the estimation of the influence of glass transition and crystallization kinetics on glass stability and potential kinetic predictions regarding the formation of far-IR optical elements and glass-ceramics.

In [77,78] was, for the first time, introduced the possibility to combine the DSC and TMA techniques with regard to obtaining the detailed information about ongoing processes connected with crystallization (which restrict the glass preparation and processing) for the whole compositional line of $Ge_{21}Se_xTe_{79-x}$ (for x up to 8 at. % of selenium) glasses [78] and one selected composition, namely the $Ge_{20}Se_4Te_{76}$ glass [77].

The combined DSC and TMA crystallization study of Ga-doped $GeTe_4$ systems is included in [70,81]. The Fig. 19 illustrates the obtained DSC and TMA crystallization curves for the selected Ge-Ga-Te compositions, where the black and red curves correspond to the data representing the two applied heating rates (1 and 10 $°C.min^{-1}$) and the vertical dashed lines then represent the actual (not extrapolated) onsets of the DSC crystallization peaks.

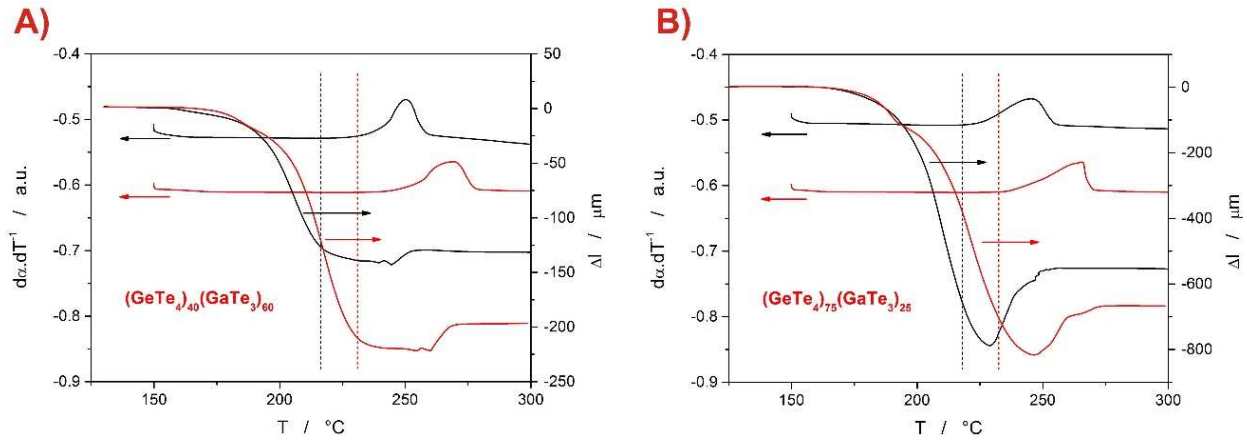

Figure 19: The comparison of DSC and TMA measurements for bulk samples of $(GeTe_4)_{40}(GaTe_3)_{60}$ (A) and $(GeTe_4)_{75}(GaTe_3)_{25}$ (B) compositions and applied heating rates 1 (black curves) and 10 (red curves) °C.min^{-1}.

The typical sample height decrease above T_g due to the rising viscous flow with increasing temperature and constant compressing force applied by TMA is apparent. The moment that crystallization occurs, the decrease of sample height stops, because the crystalline network starts to form and hinders the sample from further flow. As is evident from the comparison of DSC and TMA crystallization measurements, the cessation of TMA curve corresponds to the formation of first crystallites (the Te-precipitation). The similar findings were observed also for Se-doped GeTe glasses ([77,78]).

In the presented doctoral thesis the Hruby [28] criterion, the recently developed K_S [111-113] criterion and the next new-developed criteria called workability window and new viscous-flow-related parameter [70] will be discussed with regard to studied systems by reason they were used to determination of glass stability of all investigated glassy systems included in this thesis. The mentioned K_H and K_S criteria belong to the group of GS criteria, which are based on characteristic temperatures (T_g. T_c, T_m) and their relations. These criteria are widely used and their evaluation is very simple. Unfortunately, their outcomes are rather abstract and usually used for comparison purposes. In order to enhance this important approach, the utilization of the combined DSC and TMA crystallization data is suggested.

The Fig. 20 offers a summary of results provided by means of K_S and K_H criteria for all investigated systems. In case of $Ge_{20}Se_xTe_{80-x}$ and $Ge_{21}Se_xTe_{79-x}$ systems [75,76,78], the recently developed K_S criterion was applied to evaluation of glass stability. The data in Fig. 20 show that the glass stability of bulk materials (relevant for real-life applications) rises with the addition of selenium into GeTe matrix and get at a standstill above ~ 4 at. % of Se. The glass stability of $Ge_{21}Se_xTe_{79-x}$ system seems to be slightly better than that of $Ge_{20}Se_xTe_{80-x}$ system but not as much as was expected. The slightly higher amount of Ge, which was in case of Ge-Se-Te far-IR glasses used mainly to optimize the glass stability, did not have much impact on glass stability. However, the $Ge_{21}Se_xTe_{79-x}$ system was found as more suitable (in comparison with $Ge_{20}Se_xTe_{80-x}$) for the potential processing; the higher amount of germanium in the structure leads to slow-down of crystallization but without the influence on the position of crystallization onsets. With regard to the actual utilization of Ge-Se-Te glasses in the far-IR optics applications, it is needed to make a compromise between

the width of the transmittance window, which a little narrows with Se addition, and the glass stability, which increases with addition of selenium. The compositions with selenium content ≥ 4 at. % were found to be favorable considering the glass stability and the potential manufacture (fiber-drawing, shaping) of the glassy material. This conclusion can be also confirmed by the results from TMA analysis [77,78]. In case of the composition with 4 at. % of Se, the workability window (Eq. 25), which is defined as a temperature range between the first softening of the sample and first occurrence of crystallites, was 75 – 80 °C wide. As the selenium content increased, the workability window narrowed and for the composition with 8 at. % of selenium was 60 – 65 °C wide. These effects point to facts, that the glass-softening, viscous flow effects and occurrence of first crystallites determine the glass-stability of given materials and the correlation of DSC and TMA data can help with consideration of stability and processability of glassy materials. The $Ge_{21}Se_4Te_{75}$ glass was found as the most suitable for the further processing and applicability as a far-IR optical fibers and mold-formed optic elements.

The Hruby criterion was used for determination of glass stability of Ge-I-Te [85,86], As-Se-Te [87,88] and Ge-Ga-Te [70,79] systems. The thermal stability of $Ge_{20}I_xTe_{80-x}$ (x = 2; 5; 8; 12; 15 %) assessed on the basis of Hruby criterion was found to be fairly variable with respect to the composition and experimental conditions. The K_H values range from 0.5 to 2.5. While the glass transition temperatures and melting temperatures are invariant with regard to the sample form and heating rate, the crystallization of $Ge_{20}I_xTe_{80-x}$ glasses is largely influenced by experimental conditions. This causes the large variability of glass stability. The consideration of the influence of experimental conditions on thermal (and glass) stability of given systems is crucial. In this instance, if the bulk samples and low heating rates will be taken, the macroscopic IR optics applications (such as molded lenses) with utilization of $Ge_{20}I_xTe_{80-x}$ glasses are possible. Unfortunately from this point of view, the Se- and Ga-doped GeTe glasses are more suitable for far- IR optics applications due to the unpredictable surface precipitation of tellurium and complicated glass synthesis of I-doped $GeTe_4$ glasses. Nonetheless, the $Ge_{20}I_2Te_{78}$ glassy composition seems to be suitable for the far-IR optics ceramics and glass-ceramics due to the most pronounced transition from the pure surface to the volume-located crystal growth with the initial iodine addition.

In case of the investigated $(As_2Se_3)_{100-x}(As_2Te_3)_x$ glassy system [87,88], the eutectic-based character was observed. The position of eutectic is probably between 34 and 50 at. % As_2Te_3, this is claimed on basis of the evolution and position of the melting peaks and sub-peaks. As can be seen in Fig. 20, the glass stability for $(As_2Se_3)_{100-x}(As_2Te_3)_x$ system decreases as the As_2Te_3 content increases. The absence of crystallization process in case of 0, 17 and 34 at. % of As_2Te_3 indicates the strong glass stability, but the utilization of classic glass stability criteria (based on characteristic temperatures) fails. However, the rising glass stability with rising amount of As_2Se_3 was expected due to the fact, that the binary As_2Se_3 is well-known excellent glass-former [31,34,38,40,43-45,55-60] and also due to the presence of eutectic alloy between 34 and 50 at. % As_2Te_3.

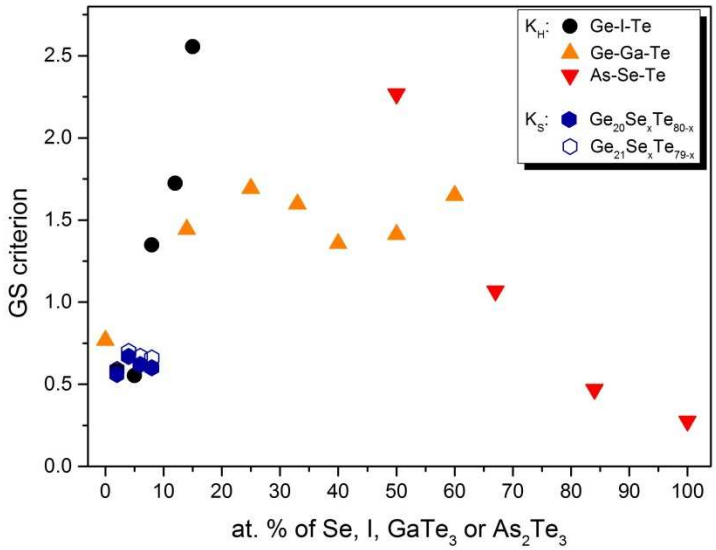

Figure 20: The compositional dependence of the evaluated GS criteria of all investigated systems for bulk samples and selected heating rate (10 °C.min^{-1}).

The Hruby criterion was applied also on $(GeTe_4)_x(GaTe_3)_{100-x}$ (x = 40; 50; 60; 67; 75; 86; 100 %) system [70,79] in order to evaluate the glass stability of investigated glasses. In Chapter 3.1, where the crystallization behavior of this system was discussed, it was found, that the crystallization onset (which determines the temperature corresponding to the first formation of crystallites) did not change with various amounts of gallium. This fact indicates the influence of T_g on resulting glass stability. As is shown in Figs. 20 and 21, on basis of results provided by Hruby criterion, the highest glass stability can be expected in case of compositions with low $GaTe_3$ content (i.e. 15 – 25 at. % of $GaTe_3$) and for the $(GeTe_4)_{40}(GaTe_3)_{60}$ compositions. Based on the findings from particle size study [79], it was found that the $(GeTe_4)_{86}(GaTe_3)_{14}$ glassy composition seems to be the most stable and impassive to the presence of structural defects and the most suitable for far-IR applications using the fully glassy materials. As far as the potential usage of this material for glass-ceramics purposes, the possible utilization of this glass (containing the low $GaTe_3$ content) is feasible due to the invariable formation of all present crystalline phases with experimental conditions, these compositions exhibited the most uniform behavior of crystallization processes. This allows the best control over the processes of crystal growth. It was also found, that the kinetics only slightly depends on applied heating rate, so that the processing of corresponding ceramics can be easier in this regard.

The Fig. 21 offers an illustration of the compositional dependence of three parameters, which can be used for the evaluation of glass stability and was applied on all investigated $(GeTe_4)_x(GaTe_3)_{100-x}$ systems. The usual way how to evaluate the glass stability of given glassy system represents the utilization of Hruby criterion (black points in Fig. 21). With respect to the limitations emerged from the nature of Hruby criterion, the newly developed parameters [33] based on the combined information provided by DSC and TMA can better serve for the GS evaluations than the commonly used Hruby criterion. The parameter called “workability window” (red points in Fig. 21) is formulated as a temperature range between the first sample height decrease arising from the viscous flow effects (TMA measurements) and the first occurrence

of crystallites (DSC measurements – the true crystallization onset). The Equation 25 is an expression of workability window (w.w.) parameter:

$$w.w. = T_{onset,DSC} - T_{flow,TMA} \tag{25}$$

As is the workability window wider, the more suitable the glass is for the next processing (fiber-drawing, molding). The information about glass stability is more exact in contrary to the standard $T_c - T_g$ difference, where the information about the glass-softening and viscous flow effects is not included.

In Fig. 21, the next parameter occurs (the blue points). This "new parameter" was introduced as a supplementary parameter to w.w. parameter, which accounts also with the rapidity of viscous flow linked to the given temperature window. The Equation 26 expresses this "new parameter" associated with the proportional decrease of sample height during the TMA crystallization measurement.

$$new\ parameter = (l_{onset,DSC} - l_{min})/(l_{max} - l_{min}) \tag{26}$$

The $l_{onset,\ DSC}$ represents the sample height at $T_{onset,\ DSC}$, l_{max} and l_{min} represent the maximum and minimum sample height during the TMA crystallization measurement. The value of the "new parameter" then corresponds to the degree of the viscous flow, which can be achieved until a moment, when the first crystallites occur. The smaller the value of this parameter, the higher viscous flow can be reached without the danger of presence of crystallization.

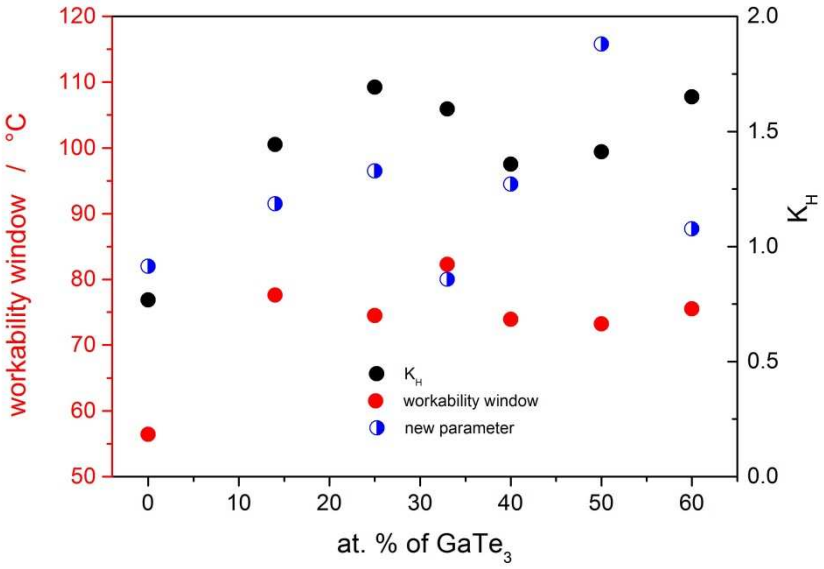

Figure 21: The compositional dependence of Hruby criterion, workability window and new-parameter for all studied $(GeTe_4)_x(GaTe_3)_{100-x}$ bulk glasses.

As was previously discussed, based on results provided by Hruby criterion, the compositions with 25 and 60 at. % of $GaTe_3$ seem to be the most stable. Nonetheless, if the next parameters (w.w. and new parameter) will be taken into account, it is apparent, that the width of workability window and the value of "new parameter" do not correspond to the K_H prediction. The better results of these new-introduced parameters are obtained for the $(GeTe_4)_{67}(GaTe_3)_{33}$ glass. This composition

is also close to the eutectic, which confirms the conclusion, that the $(GeTe_4)_{67}(GaTe_3)_{33}$ composition is probably the most suitable for the far-IR optics applications with regard to the thermal stability. Thus, the Hruby criterion was found to be less suitable for the glass-stability predictions in comparison to the new-introduced parameters.

4 Conclusions

The first goal of the doctoral thesis was the characterization of crystallization behavior of tellurium-based chalcogenide glasses, which belong to the promising materials with potential applicability in the far-infrared optics.

- The crystallization behavior of all investigated systems was characterized by means of DSC (and TMA in selected cases).
- The crystallization (and relaxation) kinetics was described by utilization of commonly used kinetic models in dependence on experimental conditions (sample form, particle size, heating rate) on account of the possibility to acquire the complete detailed information about ongoing processes. The crystallization kinetics of all investigated systems (except the $(GeTe_4)_x(GaTe_3)_{100-x}$ system) was found to be strongly dependent on applied experimental conditions due to the presence of a slightly unpredictable surface precipitation of tellurium, which determines the potential usability of these materials in real-life applications. The improvement of glass thermal properties with doping of pure Ge-Te material by selenium, gallium, iodine or with the search of optimum ratio of As_2Se_3 and As_2Te_3 contents of As-Se-Te glasses was confirmed by an extensive study of crystallization (and relaxation) behavior of whole compositional lines of all investigated systems with respect to various tested experimental conditions.
- The crystallization (and relaxation) kinetic findings were interpreted and supported by the systematic detailed structural analysis, which was performed by means of XRD analysis, Raman spectroscopy and infrared microscopy with an effort to obtain the complete thermo-structural information about the studied systems.

With regard to the observed complexity of crystallization processes of all investigated systems, this phenomenon needed to be addressed. Therefore, the second aim of the doctoral thesis was a solution of crystallization complexity by means of two approaches, i.e. the mathematic deconvolution and kinetic deconvolution procedures.

- The procedure of mathematic deconvolution of the complex kinetic signal was performed by means of Fraser-Suzuki function as the most suitable function for the non-isothermally obtained calorimetric data.
- The procedure of kinetic deconvolution was performed by means of multivariate kinetic analysis (MKA). However, this method has a certain limitation, which lies in requirement of the more-or-less constant E_A values across the whole explored range of experimental conditions. This condition was fulfilled only for the $(GeTe_4)_x(GaTe_3)_{100-x}$ system.
- Therefore, the mathematic deconvolution procedure was applied via the Fraser-Suzuki function on the remaining investigated systems.

The number of DSC curves, on which the deconvolution procedures were applied (within the work on this doctoral thesis) exceeds one thousand. Excepting the $(GeTe_4)_x(GaTe_3)_{100-x}$ system, the mathematic deconvolution was applied on all of investigated data. The mathematic deconvolution was found to be able to successfully address the issue of the temperature-dependent crystallization kinetics.

- The main purpose of this branch of this doctoral thesis was to draw an attention to this problematic and, hopefully, start off a research leading to some advancements or at least some activity regarding this issue.

The third goal of the doctoral thesis represents the utilization of the combined information obtained from crystallization measurements performed by means of DSC and TMA, results from crystallization kinetic calculations and results from a classical procedure of evaluation of glass stability of all investigated systems in order to the assessment of the suitability of studied tellurium-based glasses for the potential usage in real-life applications, such as far-IR optics, glass-ceramics, ceramics, from the thermo-kinetic point of view.

- On the basis of revealed insufficiency of classical evaluation of glass stability via Hruby criterion to correctly determine the true thermal stability of glassy material, the new approach was suggested, which is based on the combination of two thermo-analytical techniques (DSC and TMA).
- The combination of DSC and TMA crystallization measurements then offers extended information about processes ongoing in glassy materials until the moment the crystallization occurs. This area between the first softening of glass and the occurrence of the first crystallites is greatly important for the processing of the glassy material (e.g. fiber-drawing, molding, shaping) and the detailed exploration (as much as possible) can help with revelation of the behavior of the processed glass and then the experimental conditions can be exactly adjusted.
- The improvement of predictions of glass stability was proposed via the new-developed parameters (workability window and new processability parameter), which introduce an easy, fast and more accurate way of determining and tailoring the thermo-mechanical properties of glassy materials. These parameters then can serve to an effective estimation of the material's processability.

Applying the above-mentioned approaches, the Ge-Ga-Te system, namely the $(GeTe_4)_{67}(GaTe_3)_{33}$ glass was found to be the most suitable system (with respect to the thermal behavior) for the far-IR optics applications from all of the investigated systems. Also the Se-doped tellurium-based glasses were found to be suitable for the production of far-IR optic elements, namely the composition $Ge_{21}Se_4Te_{75}$. However, some limitations exist and more attention in processing of this glassy system must be paid. In case of Ge-I-Te system, the rather unpredictable surface tellurium precipitation and complicated glassy synthesis led to the Se- and Ga-doping being preferred. The most suitable glassy composition from As-Se-Te system for the far-IR optics purposes seems to be the $(As_2Se_3)_{66}(As_2Te_3)_{34}$ glass. However, this system also behaves slightly unpredictably with respect to applied experimental conditions; therefore the processing must be strictly controlled. Nonetheless, all of detected flaws can be an incentive for further deeper studies of these relatively new promising materials.

List of References

[1] P. Houizot, C. Boussard-Pledel, A. J. Faber, L. K. Cheng, B. Bureau, P. A. Van Nijnatten, W. L. M. Gielesen, J. Pereira do Carmo and J. Lucas, Opt. Exp. **15**, 12529 (2007).

[2] M. Frumar, Chemie pevných látek I, ediční středisko UPa, Pardubice (1992).

[3] P. Lucas, M. A. Solis, D. L. Coq, C. Juncker, M. R. Riley and J. Collier, Sens Actuators B **119**, 355-362 (2006).

[4] S. Maurugeon, B. Bureau, C. Boussard-Plédel, A. J. Faber, X. H. Zhang, W. Geliesen and J. Lucas, J. Non-Cryst. Solids **355,** 2074–2078 (2009).

[5] P. Houizot, C. Boussard-Plédel, A. J. Faber, L. K. Cheng, B. Bureau, P. A. Van Nijnatten, Opt Exp. **15**, 12529-12538 (2007).

[6] A. Léger, Adv. Space Res. **25**, 2209 (2000).

[7] D. Le Coq, K. Michel, J. Keirsse, C. Boussard-Plédel, G. Fonteneau, B. Bureau, J.-M. Le Quéré, O. Sire and J. Lucas, Comptes Rendus Chimie **5**, 907-913 (2002).

[8] S. Danto, P. Houizot, C. Boussard-Pledel, X. H. Zhang, F. Smektala and J. Lucas, Adv. Funct. Mater. **16**, 1847-1852 (2006).

[9] G. Wang, C. Li, Q. Nie, Z. Pan, M. Li, Y. Xu, H. Wang and D. Shi, J. Non-Cryst. Solids **463**, 80-84 (2017).

[10] C. Conseil, V. S. Shiryaev, S. Cui, C. Boussard-Pledel, J. Troles, A. P. Velmuzhov, A. M. Potapov, A. I. Suchkov, M. F. Churbanov and B. Bureau, J. Light. Technol. **31**, 1703-1707 (2013).

[11] J. A. Moon and D. T. Schaafsma, Fiber Integrated Opt. **19**, 201–210 (2000).

[12] G. Tao, H. Ebendorff-Heidepriem, A. M. Stolyarov, S. Danto, J. V. Badding, Y. Fink, J. Ballato and A. F. Abouraddy, Adv. Opt. Photon. **7**, 379-458 (2015).

[13] I. Chung and M. G. Kanatzidis, Chem. Mat. **26**, 849-869 (2014).

[14] S. Maurugeon, B. Bureau, C. Boussard-Plédel, A. J. Faber, P. Lucas, X. H. Zhang and J. Lucas, Opt Mater **33**, 660-663 (2011).

[15] S. R. Elliot, *Physics of Amofphous Materials*, Longman London, 6 (1990).

[16] P. G. Debenedetti and F. H. Stillinger, Nat. **410**, 259 (2001).

[17] C. A. Angell, K. L. Ngai, G. B. McKenna. P. F. McMillan and S. W. Martin, App. Phys. Rev. **88**, 3113 (2000).

[18] G. O. Jones, *Glass*, Methuen & Co. Ltd. London (1956).

[19] G. W. Scherer, *Glass Formation and Relaxation*, in: Materials Science and Technology **9**, edited by J. Zarzycki, VCH Weinheim, 121 (1991).

[20] J. Šesták, Měření termofyzikálních vlastností pevných látek, Academia, Praha (1982).

[21] G. Tamman, W. Hesse, Z. Anorg. Allg. Chem. **156**, 245 (1926).

[22] D. R. Uhlmann, *Advances in Nucleation and Crystallization in Glasses*, edited by L. L. Hench and S. W. Freiman, American Ceramic Soc., Columbus **91** (1972).

[23] K. A. Jackson, D. R. Uhlmann and J. D. Hunt, J. Cryst. Growth **1,** 1 (1967).

[24] D. R. Uhlmann, B. Chalmers, Ind. Eng. Chem. **57**, 19 (1965).

[25] J. J. Hammel, J. Chem. Phys. **46**, 2234 (1967).

[26] W. H. Zachariasen, J. Am. Chem. Soc. **54**, 3841 (1932).

[27] J. Zarzycki, *Special Methods of Obtaining glasses and Amorphous Materials* in: Materials Science and Technology **9**, edited by Jerzy Zarzycki, VCH Weinheim (1994).
[28] A. Hrubý, Czechoslov. J. Phys. B **22**, 1187 (1972).
[29] M. Saad and M. Poulain, Mater Sci Forum. **19**, 11 (1987).
[30] M. C. Weinberg, Phys. Chem. Glasses **35**, 119 (1994).
[31] Z. P. Lu and C. T. Liu, Acta Mater. **50**, 3501(2002).
[32] Z. Long, G. Xie, H.Wei, X. Su, J. Peng, P. Zhang and A. Inoue, Mater. Sci. Eng. **509A**, 23 (2009).
[33] P. Zhang, H. Wei, X. Wei, Z. Long and X. Su, J. Non-Cryst. Solids **355**, 2183 (2009).
[34] R. Svoboda and J. Málek, J. Non-Cryst. Solids **413** 39-45 (2015).
[35] J. Málek, Habilitační práce (1996).
[36] M. E. Brown, *Introduction to Thermal Analysis: Techniques and Applications*, Kluwer Academic Publishers (2001). ISBN 1-4020-0472-9.
[37] P. Šulcová and L. Beneš, Experimentální metody v anorganické technologii, Univerzita Pardubice, Pardubice (2002).
[38] J. Šesták, Měření termofyzikálních vlastností pevných látek, Academia, Praha (1982).
[39] S. Cui, C. Boussard-Plédel, J. Troles and B. Bureau, Opt. Mater. Express **6**, 971-978 (2016).
[40] B. Bureau, C. Boussard-Pledel, P. Lucas, X. Zhang and J. Lucas, Molecules **14**, 4337-4350 (2009).
[41] H. E. Kissinger, Anal. Chem. **29**, 1702 (1957).
[42] H. L Friedman, J. Polym. Sci. **C6**, 302 (1986).
[43] M. J. Starink, Thermochim. Acta **404**, 163-176 (2003).
[44] S. Vyazovkin, A. K. Burnham, J. M. Criado, L. A. Pérez-Maqueda, C. Popescu and N. Sbirrazzuoli, Thermochim. Acta **520**, 1-19 (2011).
[45] R. Svoboda and J. Málek, Thermochim. Acta **526**, 237-251 (2011).
[46] J. Málek and V. Smrčka, Thermochim. Acta **186**, 153-169 (1991).
[47] J. Málek, Thermochim. Acta **355**, 239 (2000).
[48] M. Avrami, J. Chem. Phys. **7**, 1103–1112 (1939).
[49] M. Avrami, J. Chem. Phys. **7**, 212-224 (1940).
[50] M. Avrami, J. Chem. Phys. **7**, 177-184 (1941).
[51] J. Šesták, *Thermophysical Properties of Solids, Their Measurements and Theoretical Analysis*, Elsevier, Amsterdam (1984).
[52] J. Málek, Thermochim. Acta **138**, 337-346 (1989).
[53] J. Málek, J. M. Criado, J. Šesták and J. Militký, Thermochim. Acta **153**, 429-432 (1989).
[54] M. E. Brown, M. Maciejewski, S. Vyazovkin, R. Nomen, J. Sempere, A. Burnham, J. Opfermann, R. Strey, H. L. Anderson, A. Kemmler, R. Keuleers, J. Janssens, H. O. Desseyn, C. R. Li, T. B. Tang, B. Roduit, J. Málek and T. Mitsuhashi, Thermochim. Acta **355**, 125-143 (2000).
[55] S. Vyazovkin and C. A. Wight, Thermochim. Acta **340–341**, 53-68 (1999).
[56] L. A. Perez-Maqueda, J. M. Criado, F. J. Gotor and J. Málek, J. Phys. Chem. A **106**, 2862-2868 (2002).

[57] L. A. Perez-Maqueda, J. M. Criado and P. E. Sanchez-Jimenez, J. Phys. Chem. A **110**, 12456-12462 (2006).
[58] J. Opfermann, J. Therm. Anal. Calorim. **60**, 641-658 (2000).
[59] C. Wagner, J. Vazquez, P. Villares and R. Jimenezgaray, Mater. Lett. **18**, 280 (1994).
[60] S. Bernard, K. Fiaty, D. Cornu, P. Miele and P. Laurent. J. Phys. Chem. B **110**, 9048 (2006).
[61] W. Weibull, J. Appl. Mech. **18**, 293 (1951).
[62] A. Perejon, P. E. Sanchez-Jimenez, J. M. Criado and L. A. Perez-Maqueda, J. Phys. Chem. B **115**, 1780-1791 (2011).
[63] R. Svoboda and J. Málek, J. Therm. Anal. Calorim. **111**, 1045-1056 (2013).
[64] R. D. B. Fraser and E. Suzuki, Anal. Chem. **38**, 1770 (1966).
[65] R. D. B. Fraser and E. Suzuki, Anal. Chem. **41**, 37 (1969).
[66] O. S. Narayanaswamy, J. Am. Ceram. Soc. **54**, 491-498 (1971).
[67] C. T. Moynihan, A. J. Easteal, M. A. Bolt and J. Tucker, J. Am. Ceram. Soc. **59**, 12-16 (1976).
[68] G. Williams and D. C. Walts, Trans. Faraday Soc. **66**, 80 (1970).
[69] R. Svoboda and J. Málek, J. Non-Cryst. Solids **378**, 186-195 (2013).
[70] R. Svoboda, D. Brandová, M. Chromčíková and M. Liška, J. Non-Cryst. Solids – in press.
[71] M. A. DeBolt, A. J. Easteal, R. B. Macedo and C. T. Moynihan, J. Am. Ceram. Soc. **59**, 16 (1979).
[72] Differential Scanning Calorimetry: First and Second Order Transitions in Polymers. www.colby.edu 2018 [cited 2018-11-12]; Available from: http://www.colby.edu/chemistry/PChem/lab/DiffScanningCal.pdf.
[73] Differential Scanning Calorimetry. www.princeton.edu 2018 [cited 2018-11-12]; Available from: http://www.princeton.edu/~achaney/tmve/wiki100k/docs/Differential_scanning_calorimetry.html.
[74] M. J. Richardson, Polymer Testing **4**, 101-115 (1984).
[75] R. Svoboda, D. Brandová and J. Málek, J. All. Compd. **680**, 427-435 (2016).
[76] D. Brandová, R. Svoboda and J. Málek, J. Non-Cryst. Solids **433**, 75-81 (2016).
[77] R. Svoboda, D. Brandová and J. Málek, J. Non-Cryst. Solids **432**, 493-498 (2016).
[78] R. Svoboda, D. Brandová, M. Chromčíková, M. Setnička, J. Chovanec, A. Černá, M. Liška and J. Málek, J. All. Compd. **695**, 2434-2443 (2017).
[79] R. Svoboda and D. Brandová, J. All. Compd. **770**, 564-571 (2019).
[80] R. Svoboda and D. Brandová, J. Therm. Anal. Calorim. **129**, 593-599 (2017).
[81] R. Svoboda, D. Stříteský, Z. Zmrhalová, D. Brandová and J. Málek, J. Non-Cryst. Solids **445-446**, 7-14 (2016).
[82] D. Brandová and R. Svoboda, J. Am. Ceram. Soc. - submitted.
[83] D. Brandová and R. Svoboda, Phil. Mag. - in press.
[84] D. Brandová and R. Svoboda, J. Am. Ceram. Soc. **102(1)**, 382-396 (2019).
[85] D. Brandová, R. Svoboda, M. Liška and J. Málek, J. Non-Cryst. Solids **475**, 121-128 (2017).
[86] S. Maurugeon, B. Bureau, C. Boussard-Plédel, A. J. Faber, P. Lucas, X. H. Zhang and J. Lucas, Opt Mater **33**, 660-663 (2011).

[87] S. Cui, R. Chahal, C. Boussard-Plédel, V. Nazabal, J. L. Doualan, J. Troles, J. Lucas and B. Bureau, Molecules **18**, 5373-5388 (2013).
[88] S. Maurugeon, C. Boussard-Pledel, J. Troles, A. J. Faber, P. Lucas, X. H. Zhang, J. Lucas and B. Bureau, J. Light. Technol. **28**, 3358-3363 (2010).
[89] B. Bureau, S. Danto, H. L. Ma, C. Boussard-Plédel, X. H. Zhang and J. Lucas, Solid State Sci. **10**, 427-433 (2008).
[90] R. Svoboda, D. Brandová and J. Málek, J. Therm. Anal. Calorim. **123**, 195-204 (2016).
[91] R. Svoboda, D. Brandová, L. Beneš and J. Málek, J. Therm. Anal. Calorim. **123**, 205-219 (2016).
[92] R. Svoboda and D. Brandová, J. Therm. Anal. Calorim. **127**, 799-808 (2017).
[93] J. Málek, Z. Zmrhalová, J. Barták and P. Honcová, Thermochim. Acta **511**, 67 (2010).
[94] Z. Zmrhalová, J. Málek, D. Švadlák and J. Barták, Phys. Status Solidi C **8**, 3127 (2011).
[95] J. Málek, Z. Zmrhalová and P. Honcová, J. Therm. Anal. Calorim. **105**, 565-567 (2011).
[96] P. Jóvári, I. Kaban, B. Bureau, A. Wilhelm, P. Lucas, B. Beuneu and D. A. Zajac, J. Phys. Cond. Matt. **22**, 404207 (2010).
[97] R. De Bastiani, E. Carria, S. Gibilisco, et. al. Phys. Rev. B **80**, 245205 (2009).
[98] O. Uemura, N. Hayasaka, S. Tokairin, T. Usuki, J. Non-Cryst. Solids **205-207**, 189-193 (1996).
[99] M. Upadhyay, S. Murugavel, M. Anbarasu, T.R. Ravindran, J. Appl. Phys. **110**, 083711-083716 (2011).
[100] M.H. Brodsky, R.J. Gambino, J.E. Smith, Y. Yacoby, Phys. St. Sol. B **52**, 609-614 (1972).
[101] E.M. Vinod, K.S. Sangunni, Thin Solid Films **550**, 569-574 (2014).
[102] A.V. Kolobov, P. Fons, J. Tominaga, et. al., J. Phys. Cond. Matt. **16**, 5103 (2004).
[103] S.S. Garje, M.C. Copsey, M. Afzaal, et. al., J. Mater. Chem. **16**, 4542 (2006).
[104] G. X. Wang, Q. H. Nie, M. Barj, X. S. Wang, S. X. Dai, X. A. Shen, T. F. Xu and X. H. Zhang, J. Phys. Chem. Sol. **72**, 5-9 (2011).
[105] C. Jiang, C. Cheng, Q. D. Zhu, X. S. Wang, Q. H. Nie, S. X. Dai, G. M. Tao, M. M. Zhu, F. X. Liao, P. Q. Zhang, X. Shen, T. F. Xu, P. Q. Zhang, Z. J. Liu and X. H. Zhang, Appl. Phys. Mater. **120**, 127-135 (2015).
[106] A. Feltz, H. J. Büttner, F. J. Lippmann and W. Maul, J. Non-Cryst. Solids **8-10**, 64-71 (1972).
[107] M. Mitkova and P. Boolchand, J. Non-Cryst. Solids **240**, 1-21 (1998).
[108] A. A. Wilhelm, C. Boussard-Plédel, Q. Coulombier, J. Lucas, B. Bureau and P. Lucas, Adv. Mat. **19**, 3796-3800 (2007).
[109] W.A. Johnson and K.F. Mehl, Trans. Am. Inst. Min. (Metall) Eng. **135**, 416-442 (1939).
[110] D. Brandová, R. Svoboda, Z. O. Zmrhalová, J. Chovanec, R. Bulánek and J. Romanová, J. Therm. Anal. Calorim. **134**, 825-834 (2018).
[111] R. Svoboda and J. Málek, J. Chem. Phys. **141**, 224507 (2014).
[112] R. Svoboda and J. Málek, J. All. Compd. **627**, 287-298 (2015).
[113] R. Svoboda, M. Kincl and J. Málek, J. All. Compd. **644**, 40-46 (2015).

List of Published Works

1. SVOBODA, Roman, BRANDOVÁ, Daniela, MÁLEK, Jiří. Thermal behavior of $Ge_{20}Se_yTe_{80-y}$ infrared glasses (for y up to 8 at. %). *Journal of Alloys and Compounds,* 2018, 680, 427-435. (**Paper I**)

2. SVOBODA, Roman, BRANDOVÁ, Daniela, CHROMČÍKOVÁ, Mária, SETNIČKA, Michal, CHOVANEC, Jozef, ČERNÁ, Andrea, LIŠKA, Marek, MÁLEK, Jiří. Se-doped $GeTe_4$ glasses for far-infrared optical fibers. *Journal of Alloys and Compounds*, 2017, 695, 2434-2443. (**Paper II**)

3. SVOBODA, Roman, BRANDOVÁ, Daniela, MÁLEK Jiří. Non-isothermal crystallization kinetics of $GeTe_4$ infrared glass. *Journal of Thermal Analysis and Calorimetry*, 2016, 123, 195–204. (**Paper III**)

4. BRANDOVÁ, Daniela, SVOBODA, Roman, MÁLEK, Jiří. Influence of particle size on crystallization and relaxation behavior of $Ge_{20}Se_4Te_{76}$ glass for infrared optics. *Journal of Non-Crystalline Solids,* 2016, 433, 75-81. (**Paper IV**)

5. SVOBODA, Roman, BRANDOVÁ, Daniela, MÁLEK, Jiří. Combined dilatometric and calorimetric study of kinetic processes occurring in $Ge_{20}Te_{76}Se_4$ infrared bulk glass. *Journal of Non-Crystalline Solids*, 2016, 432 (Part B), 493-498. (**Paper V**)

6. SVOBODA, Roman, BRANDOVÁ, Daniela, BENEŠ, Ludvík, MÁLEK, Jiří. The effect of Se ↔ Te substitution on crystallisation micro-mechanisms evincing in $GeTe_4$ glass. *Journal of Thermal Analysis and Calorimetry*, 2016, 123**,** 205-219. (**Paper VI**)

7. SVOBODA, Roman, BRANDOVÁ, Daniela. Crystallization behavior of $(GeTe_4)_x(GaTe_3)_{100-x}$ glasses for far-infrared optics applications. *Journal of Alloys and Compounds.* 2019, 770**,** 564-571. (**Paper VII**)

8. SVOBODA, Roman, BRANDOVÁ, Daniela, CHROMČÍKOVÁ, Mária, LIŠKA, Marek. Thermokinetic behavior of Ga-doped $GeTe_4$ glasses. *Journal of Non-Crystalline Solids*, in press. (**Paper VIII**)

9. SVOBODA, Roman, BRANDOVÁ, Daniela. The effect of powder coarseness on crystallization kinetics of $Ge_{11}Ga_{11}Te_{78}$ infrared glass. *Journal of Thermal Analysis and Calorimetry*, 2017, 129, 593-599. (**Paper IX**)

10. SVOBODA, Roman, STŘÍTESKÝ, Daniela, ZMRHALOVÁ, Zuzana, BRANDOVÁ, Daniela, MÁLEK, Jiří. Correlation of structural, thermo-kinetic and thermo-mechanical properties of the $Ge_{11}Ga_{11}Te_{78}$ glass. *Journal of Non-Crystalline Solids,* 2016, 445-446, 7-14. (**Paper X**)

11. BRANDOVÁ, Daniela, SVOBODA, Roman. Thermal behavior of $Ge_{20}Te_{80-y}I_y$ chalcogenide glasses (for y up to 15 at.%). *Journal of the American Ceramic Society*, submitted. (**Paper XI**)

12. BRANDOVÁ, Daniela, SVOBODA, Roman. Thermo-kinetic behavior of $Ge_{20}Te_{75}I_5$ glass for infrared optics. *Philosophical Magazine*, in press. (**Paper XII**)

13. BRANDOVÁ, Daniela, SVOBODA, Roman. Thermo-structural characterization of $(As_2Se_3)_{100-x}$-$(As_2Te_3)_x$ glasses for infrared optics. *Journal of the American Ceramic Society*, 2019, 102, 382-396. (**Paper XIII**)

14. BRANDOVÁ, Daniela, SVOBODA, Roman, LIŠKA, Marek, MÁLEK, Jiří. Thermal characterization of $(As_2Se_3)_{0.5}$-$(As_2Te_3)_{0.5}$ infrared glass. *Journal of Non-Crystalline Solids*, 2017, 475, 121-128. (**Paper XIV**)

15. BRANDOVÁ, Daniela, SVOBODA, Roman, ZMRHALOVÁ OLMROVÁ, Zuzana, CHOVANEC, Jozef, BULÁNEK, Roman, ROMANOVÁ, Jana. Crystallization kinetics of glassy materials: the ultimate kinetic complexity?. *Journal of Thermal Analysis and Calorimetry*, 2018, 134, 825-834. (**Paper XV**)

16. SVOBODA, Roman, BRANDOVÁ, Daniela. Crystal growth from mechanically induced defects. A phenomenon observed for glassy materials. *Journal of Thermal Analysis and Calorimetry*, 2017, 127, 799–808. (Paper **XVI**)

---

17. SVOBODA, Roman, SETNIČKA, Michal, ZMRHALOVÁ, Zuzana, BRANDOVÁ, Daniela, MÁLEK, Jiří, Structural interpretation of the enthalpy relaxation kinetics of $(GeTe_4)_y(GaTe_3)_{1-y}$ far-infrared glasses. *Journal of Non-Crystalline Solids*, 2016, 447, 110-116.

18. SVOBODA, Roman, BRANDOVÁ, Daniela, MÁLEK, Jiří, Crystallization behavior of $GeSb_2Se_4$ chalcogenide glass. *Journal of Non-Crystalline Solids*, 2014, 388, 46-54.

NOTES: